

---- D R A F T ----

**FRACTURE PROPERTIES AND FATIGUE CRACKING  
RESISTANCE OF ASPHALT BINDERS**

by

Arash Motamed

Anoosha Izadi

Amit Bhasin

**Research Report SWUTC/??/???????**

Southwest Region University Transportation Center  
Center for Transportation Research  
University of Texas at Austin  
Austin, Texas - 78712

January 2012

--- DRAFT ---

## **DISCLAIMER**

The contents of this report reflect the views of the authors, who are responsible for the facts and the accuracy of the information presented herein. This document is disseminated under the sponsorship of the Department of Transportation, University Transportation Centers Program, in the interest of information exchange. Mention of trade names or commercial products does not constitute endorsement or recommendations for use.

## **ACKNOWLEDGMENTS**

The authors recognize that support was provided by a grant from the U.S. Department of Transportation, University Transportation Centers Program to the Southwest Region University Transportation Center which is funded, in part, with general revenue funds from the State of Texas. The authors would like to acknowledge the help of Mr. Tim Clyne from Minnesota DOT for his help with acquiring the binder samples, binder properties and mixture performance results and Dr. Yong-Rak Kim from University of Nebraska-Lincoln, for serving as a Project Monitor for this study (one).

## **ABSTRACT**

Several different types of modifiers are increasingly being used to improve the performance characteristics of asphalt binders or to achieve desired mixture production characteristics (eg. Warm Mix Asphalt). However, current Superpave performance specifications do not accurately reflect the performance characteristics of these modified binders. The main objective of this study was to evaluate the inherent fatigue cracking resistance of asphalt binders in the form of a matrix with rigid particle inclusions. The underlying rationale for this approach was to subject the binders to a state of stress that was similar to a full asphalt mixture. This was achieved by fabricating and testing composite specimens of the asphalt binder with a gradation of different sized glass beads. Four asphalt binders with similar true temperature grades but different modifiers were used in this study. The viscoelastic and fatigue cracking characteristics of the binders were measured using the glass bead-binder composite specimens in a dynamic shear rheometer at an intermediate temperature. Results demonstrate that the four asphalt binders modified using different methods had different damage characteristics despite the fact that these four binders were rated to have very similar temperature grade based on the Superpave specifications. Fatigue cracking characteristics of the glass bead-binder test specimens used in this study were qualitatively very similar to the fatigue cracking characteristics of full asphalt mixtures using the same binders. The rank order of fatigue cracking resistance for the four glass bead-binder mixtures compared reasonably well to the rank order of fatigue cracking resistance for the full asphalt mixtures that incorporated these asphalt binders.

## EXECUTIVE SUMMARY

The asphalt pavement and materials industry has seen several emerging technologies and changes in the last decade (eg. Polymer modified asphalt binders and Warm Mix Asphalt production technology). These changes combined with an increasing emphasis on sustainability and durability of pavement materials has led to an increased use of modifiers to improve the performance or production characteristics of asphalt binders. Current Superpave performance specifications do not accurately reflect the inherent ability of the asphalt binder to resist fatigue cracking. The main objective of this study was to evaluate the inherent fatigue cracking resistance of asphalt binders in the form of a matrix with rigid particle inclusions. The underlying rationale for this approach was to subject the binders to a state of stress that was similar to a full asphalt mixture. This was achieved by fabricating and testing composite specimens of the asphalt binder with a gradation of different sized glass beads.

Four asphalt binders with similar true temperature grades but different modifiers were used in this study. The viscoelastic properties of the test specimens were measured using creep-recovery tests and frequency sweep tests. The fatigue cracking characteristics were measured using cyclic load tests with a constant stress amplitude. The linear viscoelastic properties and the results from the cyclic load tests were used with the viscoelastic continuum damage approach to estimate the fatigue life of the test specimens when subjected to a cyclic load with a constant strain amplitude.

Results demonstrate that the test method was sensitive to distinguish between the fatigue cracking resistance of the four different asphalt binders. Results also demonstrated that the four asphalt binders modified using different methods had different fatigue cracking resistance despite the fact that these four binders were rated to have very similar temperature grade based on the Superpave specifications. Fatigue cracking characteristics of the glass bead - binder test specimens used in this study were qualitatively very similar to the fatigue cracking characteristics of full asphalt mixtures using the same binders. The rank order of fatigue cracking resistance for the four glass bead - binder mixtures compared reasonably well to the rank order of fatigue cracking resistance for the full asphalt mixtures that incorporated these asphalt binders. The true failure of the test specimens occurred when the complex modulus of the specimen was much lower than 50% of its initial complex modulus. In fact, all test specimens reached 50% of their fatigue life at less than 5% of the cycles required for complete failure. This was also true of the results reported in another study using these four binders based on tests conducted on full asphalt mixtures.

--- DRAFT ---

## TABLE OF CONTENTS

<b>List of Figures</b>	<b>xi</b>
<b>List of Tables</b>	<b>xiii</b>
<b>Chapter 1. Introduction</b>	<b>1</b>
1.1 Project Background . . . . .	1
1.2 Objectives . . . . .	2
1.3 Report Structure . . . . .	2
<b>Chapter 2. Background and Research Approach</b>	<b>3</b>
2.1 The need for improved binder characterization . . . . .	3
2.1.1 Rutting resistance of asphalt binders based on MSCR test . . . . .	3
2.1.2 Fatigue and fracture properties of asphalt binders . . . . .	5
2.1.3 Moisture damage resistance of asphalt binders . . . . .	8
2.2 Methods to characterize fatigue and fracture of asphalt binders . . . . .	8
2.2.1 Test required for current PG specification . . . . .	9
2.2.2 Linear amplitude sweep (LAS) test . . . . .	9
2.2.3 Thin film fracture test . . . . .	10
2.2.4 Binder-glass bead mortar test . . . . .	10
2.2.5 Binder-fine aggregate mortar test . . . . .	11
2.3 Importance of stress state to characterize fracture and fatigue of binders . . . . .	11
2.4 Research approach . . . . .	15
<b>Chapter 3. Materials and Specimen Fabrication</b>	<b>17</b>
3.1 Selection of materials . . . . .	17
3.2 Mix preparation and sample fabrication . . . . .	17
<b>Chapter 4. Tests, Analysis and Results</b>	<b>25</b>
4.1 Tests to obtain linear viscoelastic properties and fatigue behavior . . . . .	25
4.2 Linear viscoelastic properties . . . . .	26
4.3 Results from cyclic fatigue tests . . . . .	27
4.4 Discussion of Results . . . . .	36
4.4.1 Comparison to mixture performance data . . . . .	36

4.4.2	Failure criterion . . . . .	38
4.4.3	Other notes . . . . .	39
<b>Chapter 5.</b>	<b>Conclusions</b>	<b>41</b>
<b>References</b>		<b>43</b>



## LIST OF FIGURES

Figure 2.1.	Comparison of the current PG $G^*/\sin\delta$ and proposed $J_{nr}$ parameters to determine the high temperature grade of asphalt binders . . . . .	4
Figure 2.2.	Schematic of linear undamaged properties being used to determine the tensile strength ratio for materials with similar strength; this ratio is an indicator of fatigue cracking resistance . . . . .	5
Figure 2.3.	Schematic of possible effect of modifications on strength of the material; material B will be erroneously ranked as poor if linear properties such as stiffness are used as the basis without considering strength of the material . . . . .	6
Figure 2.4.	Comparison of the current PG $G^*\sin d$ to tensile strength of asphalt binders . . . . .	7
Figure 2.5.	Comparison of energy ratio to moisture susceptibility of mixtures	9
Figure 2.6.	Setup for thin film fracture test (left) and typical stress-strain response (right) . . . . .	10
Figure 2.7.	Mortar specimen with glass bead (top left) used in a DSR (bottom left) and typical loss in $G^*$ or damage as a function of number of load cycles (right); the test can also be conducted by applying constant rate shear deformation to obtain stress-strain failure curve . . . . .	12
Figure 3.1.	Gradation of glass beads used to produce the test specimen . . . . .	18
Figure 3.2.	Assembly of the compaction mold . . . . .	20
Figure 3.3.	Addition of glass beads to asphalt binder in the temperature jacket	21
Figure 3.4.	Manually mixing glass beads with the asphalt binder to prepare a homogenous mix . . . . .	21
Figure 3.5.	Mold being filled with the loose binder-glass bead mix . . . . .	22
Figure 3.6.	Loose mix being compacted using 25 drops of a weight from a specific height . . . . .	22
Figure 3.7.	Average and standard deviation of air voids in the specimens for each one of the six binder types . . . . .	23
Figure 3.8.	Test specimen being mounted on the DSR for testing . . . . .	24
Figure 4.1.	Power law or $m$ -value for the four different mixes . . . . .	27

Figure 4.2.	Coefficient of power law or $J_1$ for the four different mixes . . . . .	28
Figure 4.3.	Typical values of $G^* \sin \delta$ for the four different mixes . . . . .	29
Figure 4.4.	Comparison of computed and measured complex modulus for different mixes and frequencies . . . . .	30
Figure 4.5.	Comparison of computed and measured phase angle for different mixes and frequencies . . . . .	31
Figure 4.6.	Range of fatigue test results for each of the four binder types . . .	32
Figure 4.7.	Typical plot showing the determination of number of load cycles to failure . . . . .	33
Figure 4.8.	Number of load cycles to failure along with maximum and minimum values from cyclic tests at 10Hz by applying a constant stress amplitude of 210 kPa . . . . .	34
Figure 4.9.	Typical damage evolution curve (C vs S) for a binder type . . . . .	36
Figure 4.10.	Fatigue cracking characteristics of full asphalt mixtures using the four different binders . . . . .	37
Figure 4.11.	Comparison of calculated number of load cycles to reach 50% of initial modulus for a cyclic test at 10Hz by applying a constant strain amplitude for binder (left) and mixture (right) . . . . .	38
Figure 4.12.	Loss in modulus as a function of number of load cycles applied for a fine aggregate matrix with unmodified PG 58-22 asphalt binder	40

**LIST OF TABLES**

Table 2.1. Summary of test methods and parameters used to characterize the  
fatigue cracking resistance of asphalt binders . . . . . 13

Table 3.1. Properties of the four modified asphalt binders used in this study . 17

Table 4.1. Sequence of loading to obtain the complex modulus of the test  
specimens . . . . . 26

--- DRAFT ---

## CHAPTER 1. INTRODUCTION

### 1.1 PROJECT BACKGROUND

A performance test to evaluate the inherent fatigue and fracture resistance of asphalt binders is required (i) as a materials selection and design tool by which to compare the inherent fatigue cracking resistance of different modified and unmodified asphalt binders, and (ii) as a purchase specification for producers who supply asphalt binders. The current performance grade or PG specification is a product of the Strategic Highway Research Program (SHRP). The specification was developed in the early 90's and was primarily based on neat or unmodified asphalt binders. In the past two decades, binder producers have incorporated polymers (eg. different types of elastomers or plastomers or combination of the two) and chemical additives such as poly-phosphoric acid (PPA) to meet the specification requirements for specific climatic and loading conditions. In addition to binder producers, contractors have increasingly started using additives such as chemical warm mix additives and liquid anti-strip agents to modify the asphalt binder to meet specific production or mixture design needs.

Three major shortcomings have emerged in the current SHRP specifications. First, the PG specification is not based on the use of modified binders. Previous studies have reported false negatives and false positives in terms of performance (D'Angelo et al., 2007; D'Angelo, 2010; Olard and Di Benedetto, 2004; Bahia et al., 2010) .

Second, the PG specification is based on properties measured at a low strain causing very little damage whereas permanent deformation and cracking occur at high levels of stress or strain. Simply stated, the use of linear viscoelastic properties for specification of asphalt binders is analogous to the use of elastic modulus (in lieu of tensile or compressive strength) for specification of materials such as steel or concrete. In fact, this shortcoming can also explain the poor correlation of the PG specification with field performance after accounting for variables due to mixture and structure design. This shortcoming has been partially resolved by introducing the multiple stress creep recovery (MSCR) test that measures the plastic deformation in asphalt binders related to rutting at the service temperature. However, there is also a need to better characterize the fatigue and fracture properties of asphalt binders at intermediate temperatures.

Third, the PG specification system does not have a provision to measure and specify the inherent resistance of asphalt binder to moisture damage. Although moisture induced

damage is a function of both the asphalt binder and aggregate, there is a need for a test and criterion that can be used to select and purchase asphalt binders for use in specific environmental conditions or use with certain aggregates.

## **1.2 OBJECTIVES**

The ultimate goal of this research project was to seek improved methods and criteria to characterize the fracture and fatigue cracking resistance of asphalt binders, particularly modified asphalt binders. As a part of this research we measured the linear viscoelastic properties of different asphalt binders using traditional rheological test methods. We also measured the strength and viscoelastic properties of asphalt binder in the form of a soft matrix with rigid particle inclusions. This was achieved by mixing the asphalt binder with relatively rigid particles of different sizes, and then testing the composite by subjecting it to different forms of loading. The tests were conducted on polymer and chemically modified asphalt binders. Finally, we also compared the results from these tests to the performance of typical asphalt mixtures that incorporate these binders to evaluate the relationship between the fatigue life of mixtures and binders to the strength and viscoelastic properties of the binders.

## **1.3 REPORT STRUCTURE**

Chapter 2 of this report presents a background on the need for improving binder specifications with an emphasis and review of the test methods that are available to characterize the fatigue and fracture properties of asphalt binders. Chapter 3 presents a description of the materials that were selected and used in this study along with a detailed description of the procedures that were used to fabricate the test specimens. Chapter 4 presents a description of the various test methods that were used with the specimens along with the detailed analysis of the test results and comparison to mixture performance. Finally, Chapter 5 presents concluding remarks based on the findings from this study.

## **CHAPTER 2. BACKGROUND AND RESEARCH APPROACH**

### **2.1 THE NEED FOR IMPROVED BINDER CHARACTERIZATION**

It is important to characterize the inherent damage resistance of asphalt binders in order to select an appropriate binder for a particular condition so as to avoid premature damage (rutting, cracking etc.) in the asphalt mixture. The ability of an asphalt binder to resist various forms of distresses is not a sufficient condition to ensure that the mixture will not experience a particular type of distress. Mixture performance is ultimately dictated by material properties (e.g. binders resistance to distresses), mixture design characteristics (e.g. gradation, aggregate quality, and binder content), environmental conditions (temperature, moisture), structural design (pavement thickness, base layer thickness), and construction quality. However, characterizing the inherent ability of the asphalt binder to resist damage is critical because: (i) it serves as a screening tool by which to select a binder that is not inherently susceptible to distresses under a given environmental and traffic loading and (ii) it serves as a benchtop tool to evaluate the efficacy of modification processes while engineering modified binders.

#### **2.1.1 Rutting resistance of asphalt binders based on MSCR test**

As per the current PG specification (AASHTO M-320), the high temperature grade of the binder is the temperature at or below which  $G^*/\sin \delta$  of the RTFO aged binder is above the specification requirement of 2,200Pa. This parameter is measured using a dynamic shear rheometer (DSR) by applying a sinusoidal loading at 10 radians/second. The high temperature grade of the binder is then used to specify and select the binder to ensure that the binder is not susceptible to rutting. The specification limit was based on straight or unmodified asphalt binders. However, in the last two decades binder producers have increasingly started using modifiers (e.g. polymers and chemical additives) to meet these specification requirements. Since the specification is based on the behavior of the binder at low strain amplitudes and does not measure the distress itself, i.e. permanent deformation, several studies have shown that the  $G^*/\sin \delta$  based specification does not correlate well with field performance (Sherwood et al., 1998; D'Angelo et al., 2007)

In subsequent work, D'Angelo and co-workers developed the multiple stress creep recovery test (MSCR) protocol to evaluate the sensitivity of asphalt binders to permanent

deformation or rutting (D'Angelo et al., 2007; D'Angelo, 2010). The test protocol requires that a 25-mm diameter and 1-mm thick asphalt specimen is subjected to 10 cycles of one second creep loading followed by 9 seconds rest period at stress levels of 100 Pa and 3200 Pa at the high PG temperature using the DSR. The three main parameters and proposed specification from this test are (i) non recoverable compliance or Jnr (permanent strain divided by the stress) computed at 3200Pa with a requirement that this value be no more than 4.0 at the high temperature, this limit is 2.0 and 1.0 when one or two grade bumps are required, respectively to accommodate for traffic volume and speed (ii) stress sensitivity computed as  $Jnr@3200Pa - Jnr@100Pa / Jnr@100Pa$  that must be less than 0.75, and (iii) the percent elastic recovery computed as  $strain@1sec - strain@10sec * 100 / strain@1 sec$  must be greater than 25% or 35% depending on traffic volume. D'Angelo et al. (2007) used ALF test section data from FHWA to demonstrate that the proposed parameter, Jnr, was much more efficient than  $G^*/sin \delta$  at detecting the resistance of the asphalt binder to permanent deformation (Figure 2.1). Reinke (2010) used Hamburg Wheel Tracking Tests (HWTT) to demonstrate that the Jnr at high stress levels was effective at screening the susceptibility of asphalt binders to rutting.

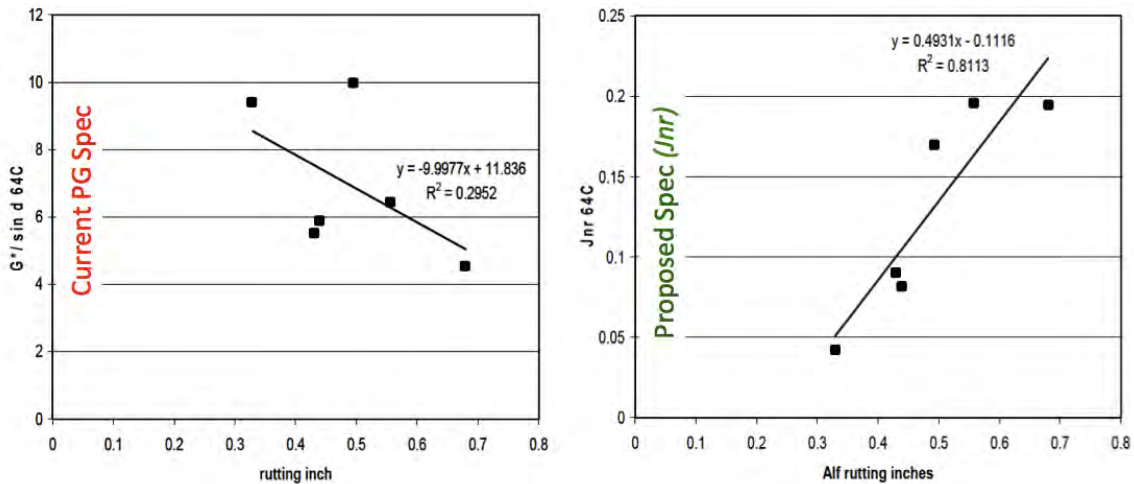


**Figure 2.1. Comparison of the current PG  $G^*/sin \delta$  and proposed Jnr parameters to determine the high temperature grade of asphalt binders**

(Adapted based on D'Angelo et al. 2007)

The aforementioned studies show promise with the use of Jnr as a parameter for performance grading of asphalt binders at high temperatures to resist rutting.



### 2.1.2 Fatigue and fracture properties of asphalt binders

According to the current PG specification (AASHTO M-320), a binder is deemed as resistant to fatigue cracking if  $G^*\sin\delta$  of the PAV aged binder is less than 5000 kPa at the intermediate temperature. In this case, intermediate temperature is defined as  $4^\circ\text{C}$  over the average of the high and low temperatures. This parameter is measured using the DSR and by applying a sinusoidal loading at 10 radians/second. Just as in the case of high temperature grade, this specification is based on neat asphalt binders. A major drawback of this specification is that it is based on stiffness of the binder and not strength of the binder. Fatigue cracking is the incremental nucleation and growth of micro-cracks. This is a fracture driven process, and therefore it is important to accurately estimate the strength of the asphalt binder in order to characterize its ability to resist fatigue cracking. More specifically, the purchase specification for asphalt binder is based on a minimum requirement for  $G^*\sin\delta$ , where  $G^*$  is the dynamic shear modulus and  $\delta$  is the phase angle. This specification is based on the premise that a stiffer asphalt binder is more susceptible to fatigue and low temperature cracking. This premise implicitly assumes that all asphalt binders have similar tensile strength.

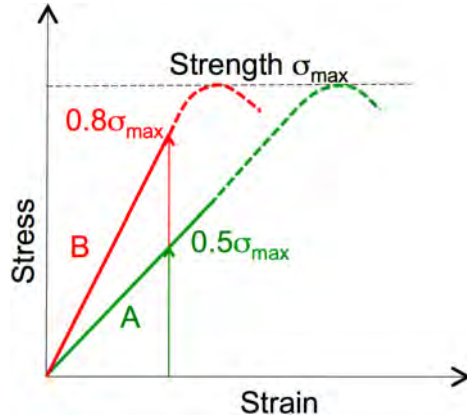


**Figure 2.2. Schematic of linear undamaged properties being used to determine the tensile strength ratio for materials with similar strength; this ratio is an indicator of fatigue cracking resistance**

As a simplified analogy, Figure 2.2 illustrates two different materials with similar tensile strength. In this case, when both materials are subjected to the similar tensile strains, the material with higher stiffness would result in a higher stress to strength ratio. Consequently, the material with the higher stiffness would be more prone to fatigue cracking. The rationale for using the current specification criterion for asphalt binders is somewhat sim-

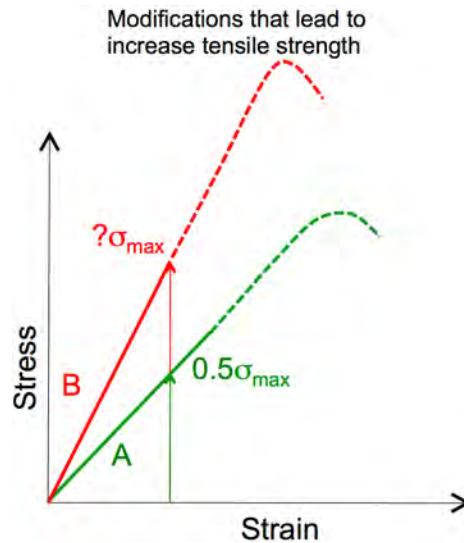


**Figure 2.3. Schematic of possible effect of modifications on strength of the material; material B will be erroneously ranked as poor if linear properties such as stiffness are used as the basis without considering strength of the material**

ilar. However, the SHRP research was conducted on mostly unmodified asphalt binders. Over the last two decades, asphalt binder producers have started producing asphalt binders using chemical and physical modifiers (e.g. poly phosphoric acid and polymers). In addition, users of the asphalt binders have increased the use of other modifiers such as liquid anti strip agent for moisture resistance and waxes and surfactants to produce warm asphalt mixtures. Several of these modifications are likely to modify the strength properties of the asphalt binder as well. Consequently, the linear elastic or viscoelastic properties of the binder are unlikely to be an accurate reflection of the strength of the material (Figure 2.3).

Bahia et al. (2010) reported a poor correlation between  $G^* \sin \delta$  and fatigue cracking of HMA pavements. Similar findings were reported by other researchers along with suggested alternatives to replace the  $G^* \sin \delta$  as a specification for resistance to fatigue crack growth (Olard and Di Benedetto, 2004; Andriescu and Hesp, 2009). In a recent study, Arega et al. (2011) measured  $G^* \sin \delta$  for several different modified and unmodified binders including binders that were modified using WMA additives. They compared this to the tensile strength of the asphalt binders and showed that there was very little correlation between stiffness and tensile strength of the asphalt binder (whereas the latter is directly related to fatigue crack growth). In fact, in many cases, tensile strength of the binder increased with an increase in stiffness suggesting an improvement in the fatigue cracking resistance when subjected to similar stress conditions. However, it is clear from the results that certain

binders that very easily met the specification limit for  $G^*\sin\delta < 5000$  kPa had a very low tensile strength as well and vice-versa (Figure 2.4).

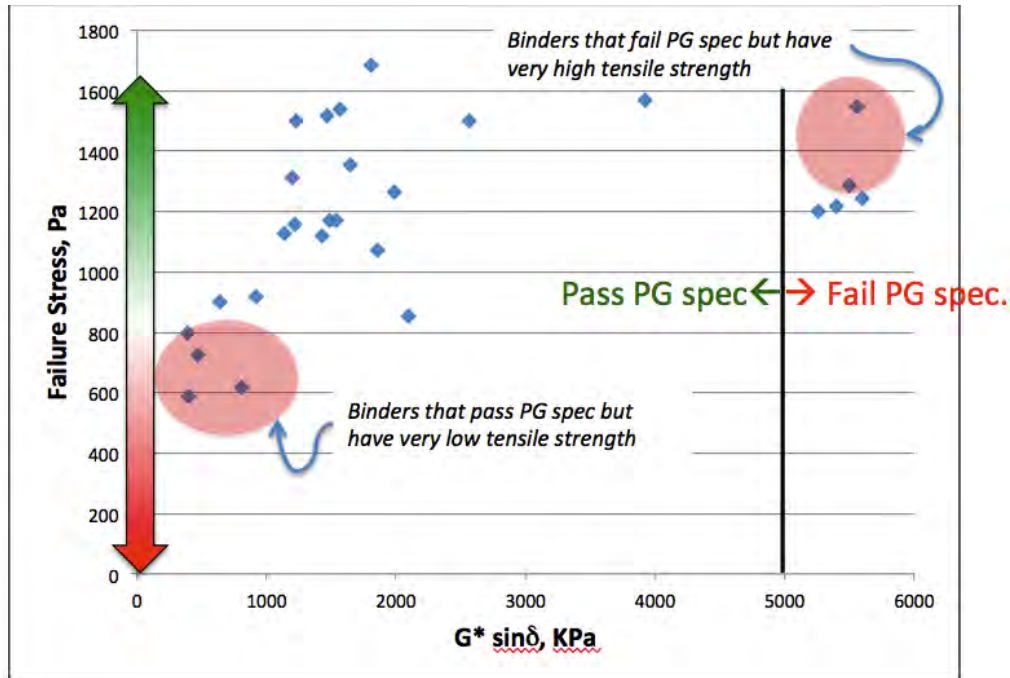


**Figure 2.4. Comparison of the current PG  $G^*\sin\delta$  to tensile strength of asphalt binders**

Ongoing studies attempt to rectify the shortcomings of the  $G^*\sin\delta$  using other approaches to test the asphalt binder with a dynamic shear rheometer (DSR). Two approaches in particular are the time sweep test and the amplitude sweep test. Anderson et al. (2001) reported that the use of a DSR for a time sweep test on asphalt binder specimens in a parallel plate geometry may result in artifacts that may resemble fatigue failure. Subsequently, Planche et al. (2004) reported that several artifacts that look like fatigue damage in the mechanical response can be corrected to obtain the true fatigue behavior of the asphalt binder. Bahia and co-workers have proposed the linear amplitude sweep test (LAS) to measure the fatigue cracking resistance of asphalt binders. The test requires that a sample of the binder be subjected to sinusoidal loading in the DSR (similar to the current method). After a specific number of cycles the applied stress amplitude is increased and process is repeated until the stress amplitude is high enough to cause damage to the specimen. Johnson (2010) conducted the LAS test on materials from several LTPP test sections and compared the results to the amount of cracking observed in the pavement. The results were promising despite the fact that differences in strain levels due to differences in pavement structures would

also play a role in the overall cracking observed in the pavement sections. The subsequent section presents a more detailed review of the various methods that have been developed to characterize the fatigue and fracture properties of asphalt binders.

### **2.1.3 Moisture damage resistance of asphalt binders**

Moisture damage is a function of both the aggregate and asphalt binder and as such an isolated binder specification for moisture damage may not be efficient. Despite this limitation, it is possible to propose a specification test and requirement for generally basic (e.g. limestone) and acidic aggregates (e.g. siliceous). In a previous studies an energy ratio parameter was proposed to differentiate and screen combinations of asphalt binders and aggregates that were susceptible to moisture induced stripping (Bhasin et al., 2006). Figure 2.5 illustrates this ratio for eight different mixtures, three of which had reported poor moisture damage resistance. Although computing the energy ratio requires measuring the surface free energy values of both the binder and the aggregate, it is possible to only measure the values of the asphalt binder and use values for the surface energy of the aggregate (or a similar aggregate) from a database of values that is already available. This study also demonstrated that there is greater variability in the surface free energy of asphalt binder as compared to the surface free energy of the aggregate.

Other measures for moisture sensitivity of asphalt binders include conducting binder fracture tests under submerged condition and the PATTI (Pneumatic Adhesion Tensile Test Instrument) test. The PATTI test is a quality control test used in the adhesives and coatings industry and measures the ability of an adhesive agent or coating to bond to a substrate. In the context of asphalt binders and mixtures it can be used to measure the adhesive bond strength of the asphalt binder to a standard substrate such as glass or an aggregate substrate. The test can be conducted with or without moisture conditioning to evaluate the adhesive bond strength of the mix.

## **2.2 METHODS TO CHARACTERIZE FATIGUE AND FRACTURE OF ASPHALT BINDERS**

There is currently some work that has been done to improve the current intermediate temperature PG specification (AASHTO M-320) for the fatigue cracking resistance of the asphalt binder. A brief description of some of these test methods is presented below.

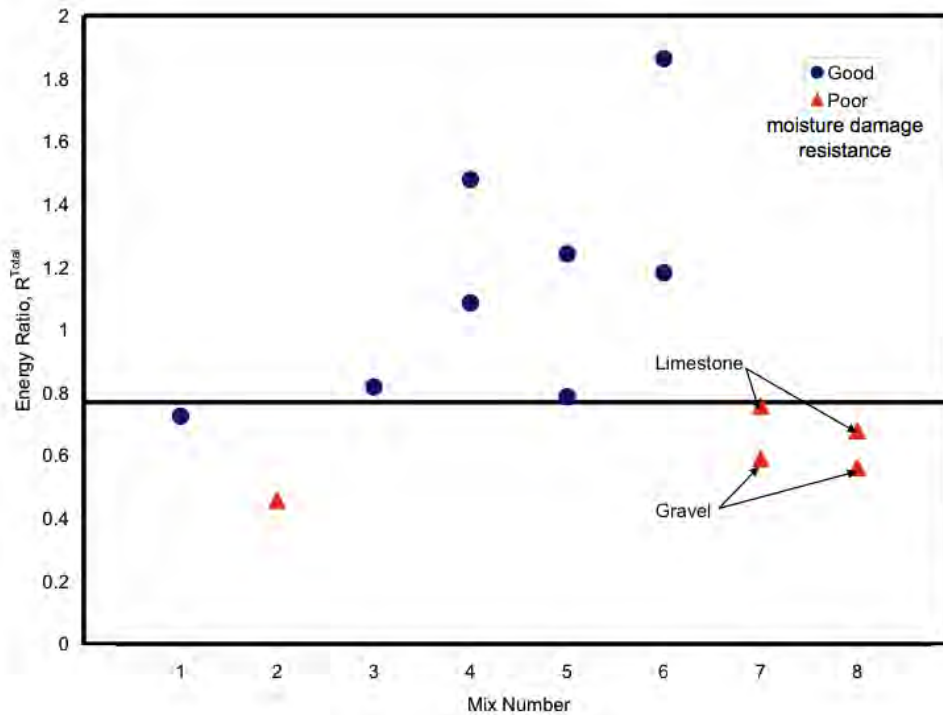


**Figure 2.5. Comparison of energy ratio to moisture susceptibility of mixtures**

### 2.2.1 Test required for current PG specification

The current PG specification requires that the complex modulus and phase angle of the asphalt binder be measured at intermediate temperatures using the DSR. This information is then used to qualify the asphalt binder for use at intermediate temperatures by specifying an upper limit for the value of  $G \cdot \sin \delta$ .

### 2.2.2 Linear amplitude sweep (LAS) test

This test is typically conducted by applying a strain controlled cyclic load to a 1 mm thick binder specimen between parallel plates using the DSR. The applied strain amplitude is linearly increased after every 100 cycles. The resulting shear stress is recorded and analyzed to quantify the fatigue cracking potential. A creep-recovery test or a frequency sweep test at low stress or strain amplitudes is also typically conducted prior to the LAS in order to obtain the linear viscoelastic properties of the binder. The linear viscoelastic properties are then used along with the data obtained from the LAS to compute the damage parameters.

### 2.2.3 Thin film fracture test

Both the linear amplitude sweep test and the monotonic fracture test are conducted on bulk specimens of asphalt binders. In real asphalt mixtures, asphalt binder is confined between relatively rigid aggregate particles. This confinement results in very high hydrostatic stresses and significantly improved tensile strength similar to thin films of adhesives between rigid substrates. As a result, it is important to consider the stress state of the asphalt binder when subjecting it to a fatigue or fracture test. The thin film fracture test is a direct tension test that is conducted on a thin film of asphalt binder.

In this test a constant rate (monotonic) displacement is applied in direct tension on a thin film of asphalt binder between two metal substrates until failure. The test can be conducted using different rates of loading and the load versus deformation curve can be used to characterize the inherent fracture resistance of the asphalt binder. This test can also be conducted using cyclic loading to simulate fatigue cracking in the asphalt binder specimen. Figure 2.6 illustrates the test set up and a typical load versus deformation curve along with the maximum load to failure.

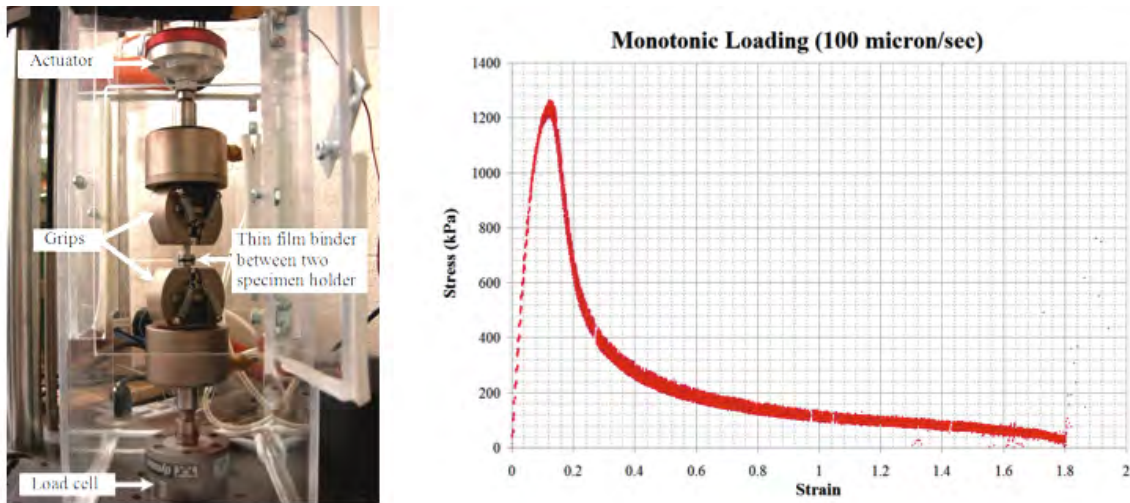


Figure 2.6. Setup for thin film fracture test (left) and typical stress-strain response (right)

### 2.2.4 Binder-glass bead mortar test

The stress state that the binder experiences in the mixture can also be simulated in a mortar specimen, i.e., binder mixed with sand sized and finer aggregates. However, it is also

important to avoid the influence of aggregates in trying to evaluate the inherent fracture resistance of asphalt binders. This is especially true if the test is to serve the purpose of a binder purchase specification in future. Therefore, this utilizes a standard material such as glass beads to fabricate the mortar specimen.

In a typical test, the mortar specimen is fabricated using a mixture of asphalt binder and glass beads of various sizes. Figure 2.7 illustrates a typical mortar specimen from a recent proof-of-concept study conducted by the researchers. The specimen uses glass beads of sizes 1mm, 0.5mm, and 0.1mm following close to dense graded line. The test can be conducted by applying either a monotonically increasing shear stress or cyclic loading with constant stress or strain amplitude. Figure 2.7 illustrates the typical results when a cyclic load is applied. Since the fatigue damage in this specimen occurs in a composite that can be treated as a continuum, the viscoelastic continuum damage (VECD) principles can also be used to extract the true fatigue characteristics of the specimen irrespective of the rate of loading and mode of loading (continuous or cyclic). Researchers have successfully used this theory in other ongoing projects.

### **2.2.5 Binder-fine aggregate mortar test**

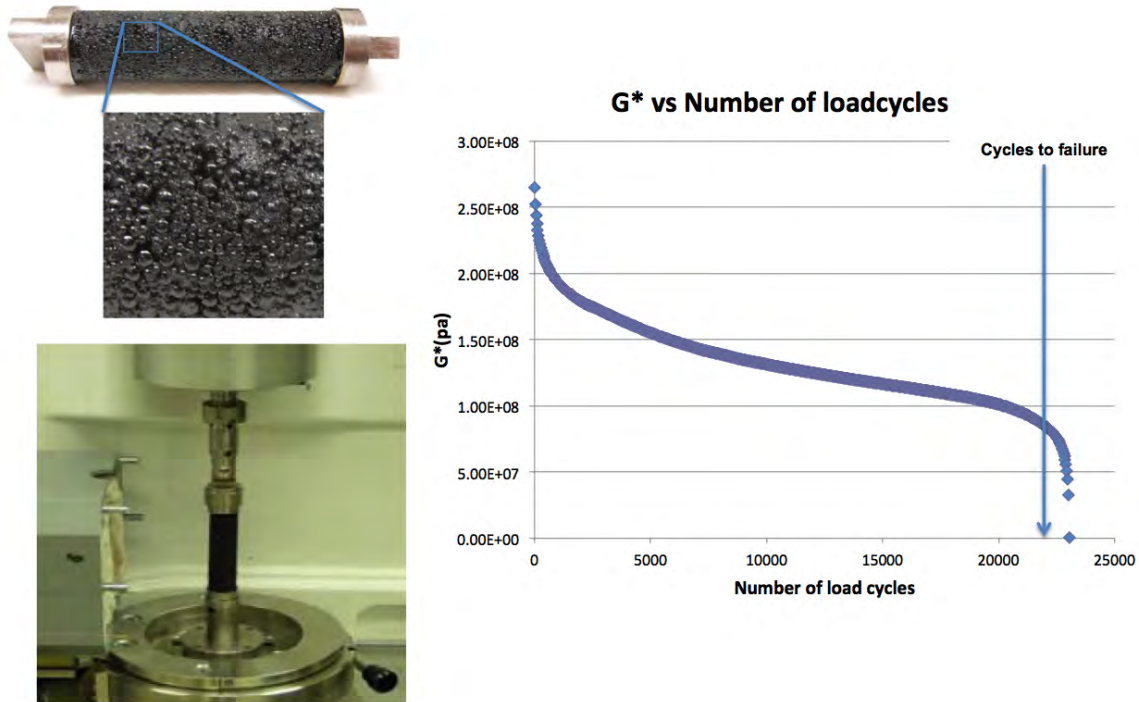
This test is the same as the binder-glass bead mortar test, except that the glass beads are replaced with the mineral aggregates corresponding to a specific asphalt mixture.

Table 2.1 summarizes the different test methods and parameters associated with these test methods that can be used to characterize the fracture and fatigue cracking resistance of asphalt binders.

## **2.3 IMPORTANCE OF STRESS STATE TO CHARACTERIZE FRACTURE AND FATIGUE OF BINDERS**

The failure mechanism of asphalt binder or mastic within an asphalt mixture cannot be considered in isolation without considering the stress state of the material. A typical asphalt mixture is a composite with a relatively soft matrix (asphalt binder or mastic) that binds rigid particles (aggregates) together. High hydrostatic tensile stresses can develop in the matrix when the mixture is subjected to tension. Therefore it is imperative that the fracture properties of the matrix (binder or mastic) are investigated under a similar state of stress.

One of the test configurations that allows testing of asphalt binders under such a stress state is the transverse tensile testing of thin films of asphalt. In fact, the relevance of film



**Figure 2.7. Mortar specimen with glass bead (top left) used in a DSR (bottom left) and typical loss in  $G^*$  or damage as a function of number of load cycles (right); the test can also be conducted by applying constant rate shear deformation to obtain stress-strain failure curve**

thickness to asphalt mixture performance has been qualitatively recognized for over 80 years with the introduction of this concept in mixture design by Hveem in the 1930s. Another example is study by Li et al. (2009) that demonstrated the relationship between film thickness and mixture rutting. It is also noteworthy that recent studies (Elseifi et al., 2008) have demonstrated that the film thickness varies greatly within an asphalt mixture specimen and also around an aggregate particle within the mixture. Elseifi et al. (2008) concluded that there is no “film” of asphalt binder as such that coats the aggregates in an asphalt mixture. In light of these studies, one may argue the applicability of testing thin films of the asphalt binder to mixture performance. This apparent contradiction is resolved considering the fact that the stress state of the asphalt binder in a thin film subjected transverse tension (in particular the hydrostatic tensile stresses) are similar to the stresses experienced by the asphalt binder in a mixture. For example, Hom and McMeeking (1991) analyzed the state of stress in a composite of rigid particles surrounded by a thin film of a relatively softer matrix. They demonstrated that the thin layer of the matrix between the rigid particles can



**Table 2.1. Summary of test methods and parameters used to characterize the fatigue cracking resistance of asphalt binders**

Test Protocol / Method	Parameters
Complex modulus using DSR and stiffness using BBR (AASHTO M-320)	Complex modulus
	Phase angle
	True low temperature grade
	S and m value for the binder
Linear Amplitude Sweep (LAS) in shear	Slope of the modulus versus damage curve
	A35 parameter (as proposed by previous researchers), i.e. the damage intensity corresponding to a 35% decrease from the initial value of $G^*\sin\delta$
Thin film fracture test in direct tension	Maximum stress to fracture for continuous or monotonic loading
Binder-glass bead mortar test	Strain energy to fracture for continuous or monotonic loading
Binder-fine aggregate mortar test	Dissipated strain energy to fracture for cyclic loading
	Number of cycles to failure for cyclic loading

develop extremely high hydrostatic stresses far exceeding the uniaxial tensile strength of the matrix. In another study, Fond (2001) reported the high hydrostatic stresses at the poles of a rigid spherical inclusion in a soft matrix that eventually results in failure initiation or propagation starting at this location. Studies conducted on asphalt binders and other similar materials subjected to such a stress state are briefly discussed below.

Gent and Lindley (1959) were amongst the first few researchers to perform experiments on a thin film of a soft elastic material between rigid substrates; now commonly referred to as the poker chip geometry. Their objective was to create a high hydrostatic tensile stress to initiate failure at the center of the test specimen. Based on these tests they demonstrated that the critical hydrostatic tensile stress resulting in failure was a material property that was closely related to the elastic modulus of the material. Their work was further extended by Lindsey (1967) who also demonstrated that high tensile hydrostatic stresses are developed in confined thin films. Lindsey used the solution for stress field in a poker chip geometry to compute the critical hydrostatic tensile stresses in the thin film at the point of failure. His results demonstrate that under high such conditions, the failure strain of the material was approximately 10 times smaller than the failure strain from a uniaxial tensile test and that the hydrostatic tensile stresses were two to three times the tensile stresses from uniaxial tensile tests. Based on the previous work of Fisher, Lindsey (1967) reinforced the idea that

the critical hydrostatic tensile stress at which material failure initiates is a material property. More recently, Cristiano et al. (2010) hypothesized that the critical hydrostatic tension at which failure occurs can be treated as a material property (consistent with Lindsey) as long as the size and distribution of inherent defects or flaws within the material did not change. In their experiments, Cristiano et al. (2010) created a hydrostatic stress state in a soft polymeric material using a thin film of the soft material between a glass sphere and a flat plate. They also demonstrated that the critical hydrostatic tensile stress at which failure initiates was a material property that was related not only to the modulus of the material (as proposed by Gent and Lindley in 1959) but also to its fracture energy.

In the context of asphalt binders and mastics, Marek and Herrin (1968) evaluated the effects of loading rate, temperature, and film thickness on the tensile behavior and failure characteristics of thin asphalt films. They measured the tensile failure in thin films of asphalt binders constrained between rigid plates (the poker chip geometry). They varied the film thickness in their experiments and noted that, at a given temperature and rate of loading, the mode of failure transitioned from fracture to a flow type failure with an increase in the thickness of the asphalt film. Harvey and Cebon (2003) used both direct tension tests on thin films and a double cantilever beam to evaluate the fracture properties of an asphalt binder at different temperatures and strain rates. They emphasized the importance of the hydrostatic stress state in thin films that ultimately influences the failure mechanism in asphalt binders. Their results demonstrate that in the case of thin asphalt films with an aspect ratio of 8 or more, the failure mode was predominantly brittle fracture and the failure strain and fracture energy did not change significantly at different rates of loading. Masad et al. (2010) evaluated the influence of film thickness, rate of loading and theoretical work of fracture on the measured fracture properties of thin asphalt films. Their results were consistent with the findings reported by Marek and Herrin (1968). Poulidakos and Partl (2010) evaluated the influence of binder type, moisture and temperature on the fracture properties of thin asphalt films. They used asphalt binder films that were 20 micrometer thick in a geometry with an aspect ratio of 250. Although the film thickness was used as a variable, the authors emphasized the importance of testing thin films that provide a more realistic representation of the stress state of the asphalt binder or mastic within an asphalt mixture.

The main objective of this study was to evaluate the fatigue cracking characteristics of four different modified binders when subjected to a stress state similar to what the binder experiences in an asphalt mixture. The aforementioned studies clearly highlight the impor-

tance of the stress state of the binder while evaluating its fracture properties. One way to achieve this is by subjecting thin films of asphalt binder to transverse tension (monotonic or cyclic) using a poker chip geometry. This approach is extremely sensitive to the uniformity of thickness of the test specimen, defects at the substrates, and alignment of the specimen in the loading frame. The authors have successfully used this geometry in previous work (Arega et al., 2011) to assess the impact of asphalt additives on its fracture properties. However, in this study the desired stress state was achieved by preparing a composite using the asphalt binder and glass beads of three different sizes. Further details on the choice of gradation, binder content, and specimen fabrication are presented in the following chapter.

## **2.4 RESEARCH APPROACH**

The focus of this research was to develop a test method that evaluates the fatigue cracking resistance of asphalt binders. The proposed test method will be developed based on the recognition that the stress state of the asphalt binder within the mixture has a significant influence on the mode of failure. In particular, for this study the binder-glass bead mortar test was fully developed and employed to test the fracture properties of four modified asphalt binders. The tests were conducted using different modes of loading and the results were compared to available data from the testing of full asphalt mixtures.

--- DRAFT ---

## CHAPTER 3. MATERIALS AND SPECIMEN FABRICATION

### 3.1 SELECTION OF MATERIALS

Four modified asphalt binders were selected for this study. The binders were provided by Minnesota Department of Transportation from the MnRoad project. The four binders had very similar true grades based on the current performance grading system. However, these four binders were produced by modifying a PG 58-34 binder using different additives. Table 3.1 presents the information on these four binders. Additional information on these binders can be found in elsewhere in the literature (Fee et al., 2008).

**Table 3.1. Properties of the four modified asphalt binders used in this study**

Property / Binder Label	P	S	PS	PE
Modification Type	PPA	SBS	PPA + SBS	PPA + Elvaloy ®
Weight % of Modifier	0.75	2.0	0.3 + 1.0	0.3 + 1.0
High Temperature Grade	62.1	62.5	62.1	62.7
Low Temperature Grade	-35.7	-35.5	-34.8	-35.1
MnRoad Reference	33	34	35	77-79

These binders were used with hydrated lime in the MnRoad test sections. A liquid anti-strip agent was also used in three of the four mixtures. It is noted that although the addition of hydrated lime or liquid anti-strip agent could possibly influence the fracture properties of the binder within the mix, these additives were not included at this stage of this study.

The only other material that was used for these tests were glass beads of different sizes. Recall that the objective of this study was to evaluate the inherent fracture and fatigue characteristics of the asphalt binder. Three different sizes of the glass beads were used to create a gradation that closely follows the maximum density line on a 0.5 power chart (Figure 3.1).

### 3.2 MIX PREPARATION AND SAMPLE FABRICATION

The four asphalt binders used in this study were aged using the rolling thin film oven (RTFO) to simulate short-term aging and the pressure aging vessel (PAV) to simulate long-term aging. The RTFO aging was carried as per ASTM D2872, where 35 grams of the binder was poured into the RTFO bottles, and aged in the RTFO for 85 minutes. The

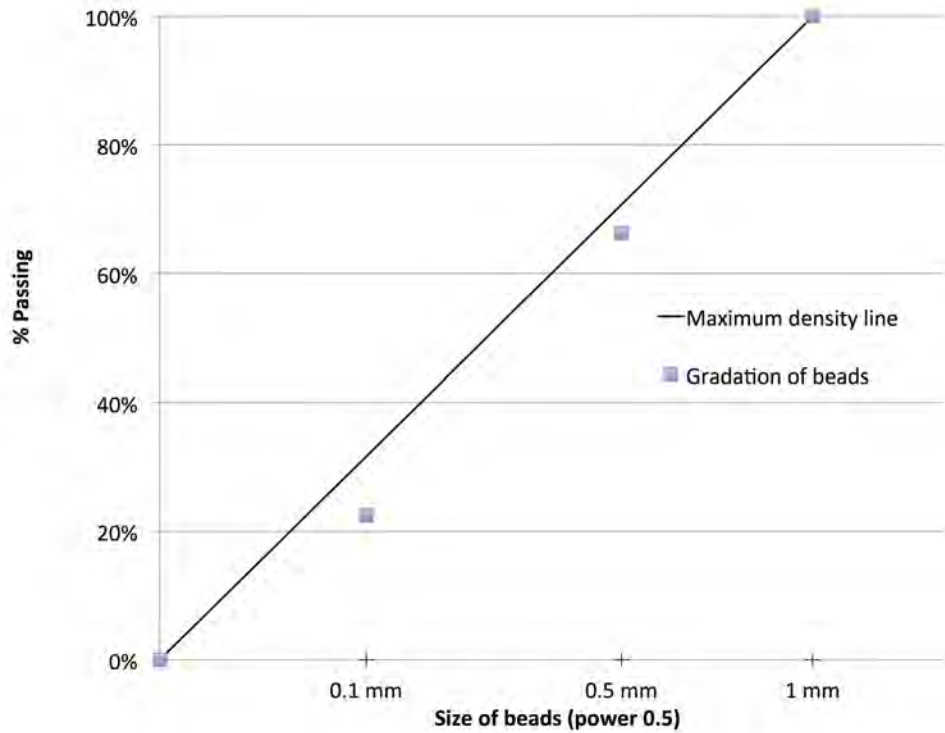


**Figure 3.1. Gradation of glass beads used to produce the test specimen**

RTFO aged binder residues were further aged in the PAV to simulate long-term aging of the binders. The PAV aging process was carried out as per ASTM D6521, where 50 grams of the RTFO residue was poured into the PAV pans and aged in the PAV for 20 hours at a temperature of 100°C (212°F).

The three different sizes of glass beads used in this study corresponded to the gradation shown in Figure 3.1. The optimal binder content was determined by trial and error. Specimens prepared using 10% binder by weight of the glass beads were found to be optimal. In this study, the 10% binder content was determined based on trial and error. Mixes were prepared and compacted using several different binder contents. Compacted specimens with low asphalt binder contents were found to be too brittle and susceptible to breakage during handling and specimen preparation. On the other hand, specimens with high asphalt binder contents were found to have problems related to flushing and deformation. A more thorough investigation of the binder content and its influence on the stress-state when used as a matrix with glass beads as an inclusion was beyond the scope of this study and is warranted for future work.

The following procedure was used to prepare the asphalt binder-glass bead mix. The asphalt binder was heated to 150°C in a 100 g can enclosed in a temperature controlled jacket. A thermocouple was used to constantly monitor the temperature of the binder throughout the process. The appropriate amount of glass beads were weighed in advance and oven dried. Once the binder reached the target temperature, the glass beads were slowly added to the binder while constantly stirring the mix in the temperature jacket. The mixing was done by adding glass beads of each size at a time, starting from the smallest to the largest size (0.1 mm, 0.5 mm and 1 mm). The beads and the asphalt binder were thoroughly mixed manually until a homogenous mix was obtained (Figures 3.3 and 3.4). After mixing the contents were transferred to an aluminum mold to compact and produce test specimens.

A two piece aluminum mold was fabricated to compact and prepare the test specimens. The mold had a total height of 75 mm and internal diameter of 12.5 mm. The mold also had a stop at the bottom and the compaction rod at the top was designed to allow dropping a fixed weight (335 g) from a fixed height (75 mm). The two pieces of the mold were held together using two pipe clamps. A total of three molds were fabricated to be able to fabricate three test specimens using the loose mix at the same time and minimize the amount of reheating required.

In order to prepare the test specimens, the molds were heated in a convection oven to 150°C. Prior to placing in the oven, each two piece aluminum mold was disbanded and the insides of the aluminum molds were sprayed with a silicon lube. The molds were then reassembled and placed in the oven. The silcion spray was used to aid removal of the sample from the aluminum mold. The compaction rod was also placed in the oven along with the molds. When the loose mix was ready the molds were removed from the oven one at a time. The loose mix was filled in the mold about two-thirds of the way full (Figure 3.5). The loose mix was then compacted using the compaction rod and dropping the weight from a fixed height 25 times. Several trials were conducted by compacting the specimen in two or three layers. In most cases, the result was that a weak interface was formed when a layered approach to compaction was used. This resulted in the test specimens failing along a horizontal plane at the interface. Annealing the test specimen to eliminate the weak interface was only partially effective. After several trials it was decided that only a single layer and compaction would be used. Trials were also conducted to determine the number of drops required to compact the sepcimen. Based on these trials it was determined that the specimen height did not change after 25 drops (Figure 3.6).

The compacted specimens were allowed to cool to room temperature in the molds for



**Figure 3.2. Assembly of the compaction mold**

24 hours. After this time the clamps holding the two piece mold were removed. The bottom of the mold was removed and two halves of cylindrical mold were then gently pried open to extract the specimen. In some cases the specimens remained adhered to the mold. In such cases, a blow torch was used for about 5 to 10 seconds to gently warm the surface of the mold. This facilitated the removal of the specimen. The ends of the final test specimen were trimmed using a tile saw such that the final height of the specimen was 50 mm.

The volume percent of air voids in each specimen was measured using the following procedure. The dry weight of the specimen ( $W_{dry}$ ) was measured using a balance with a





**Figure 3.3. Addition of glass beads to asphalt binder in the temperature jacket**



**Figure 3.4. Manually mixing glass beads with the asphalt binder to prepare a homogenous mix**

resolution of 0.1 mg. The specimen was then weighed in water ( $W_{wet}$ ), surface dried with a cloth and weighed again to obtain the saturated surface dry weight ( $W_{SSD}$ ). The bulk specific gravity of the specimen was determined as follows:



**Figure 3.5. Mold being filled with the loose binder-glass bead mix**



**Figure 3.6. Loose mix being compacted using 25 drops of a weight from a specific height**

$$G_b = \frac{W_{dry}}{W_{SSD} - W_{wet}} \quad (3.1)$$

The maximum specific gravity of the specimen ( $G_{mm}$ ) was determined as follows:

$$G_{mm} = \frac{100 + P_b}{\frac{100}{G_{se}} + \frac{P_b}{G_b}} \quad (3.2)$$

where,  $P_b$  is the percentage by mass of binder in the total mixutre,  $G_b$  is the specific gravity of the binder (considered to be 1 in this case), and  $G_{se}$  is the effective specific gravity of the glass beads (2.5 in this case based on manufacturer specification). The maximum specific gravity was used to determine the percentage of air voids in each specimen by measuring its bulk specific gravity. For all the specimens included in this study the air voids were within  $15 \pm 1.5\%$ . Figure 3.7 presents the average air voids in the specimens for each mix type along with one standard deviation.

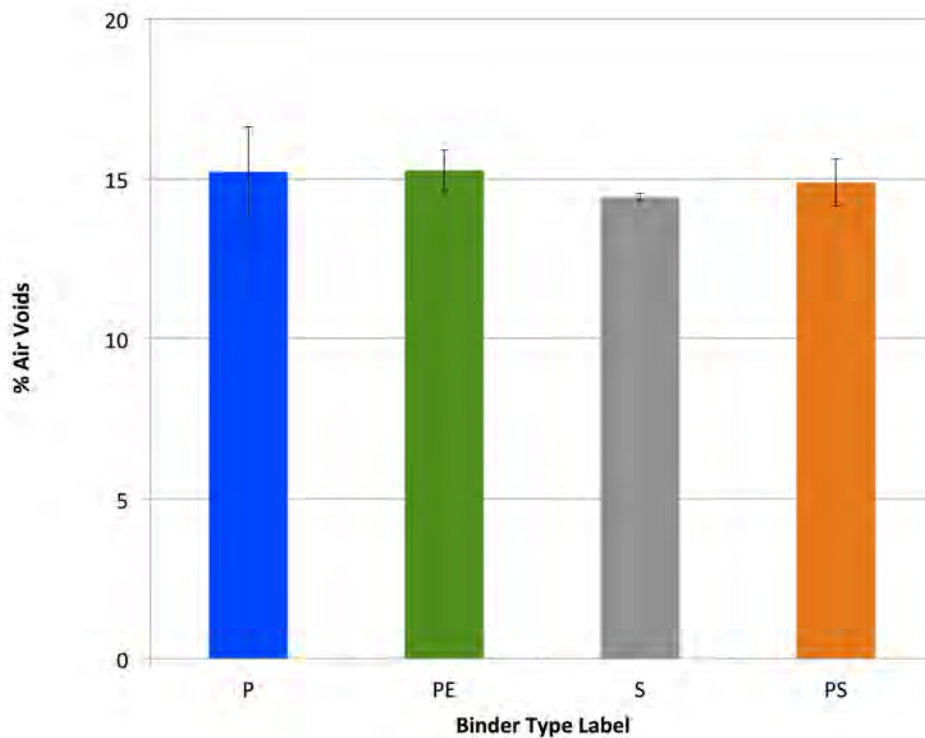


**Figure 3.7. Average and standard deviation of air voids in the specimens for each one of the six binder types**

Once the air voids of the test specimen were determined, the ends of the specimen were

then glued to metal end caps using high strength epoxy. After the high strength epoxy set completely, the test specimen was mounted onto a DSR for further testing (Figure 3.8). A total of six specimens for each of the four binder types were fabricated and tested.



**Figure 3.8. Test specimen being mounted on the DSR for testing**

## **CHAPTER 4. TESTS, ANALYSIS AND RESULTS**

The two main objectives of the tests conducted using the DSR were to obtain the linear viscoelastic and fatigue properties of the glass bead specimens subjected to torsional shear. The following are some more details pertaining to the tests conducted using the DSR. All tests described in this section were conducted at an intermediate temperature of 16°C. The test specimens were mounted in the DSR and were allowed to rest for at least 30 minutes to ensure that the test specimens had come to thermal equilibrium at the test temperature.

### **4.1 TESTS TO OBTAIN LINEAR VISCOELASTIC PROPERTIES AND FATIGUE BEHAVIOR**

All test specimens were subjected to a creep-recovery test as well as a cyclic test to obtain the linear viscoelastic properties. The linear viscoelastic properties used in the analysis and reported in this study correspond to three of the six specimens for each binder type that were tested. This was because for the first three specimens, the tests were conducted at a much lower stress magnitude which resulted in very small strains that were very close to the resolution of the instrument. Consequently, it was decided to use slightly higher stress magnitude for the latter three specimens of each asphalt binder. The following sequence of loads were used to obtain the linear viscoelastic properties.

A creep load was applied for 2 seconds at a shear stress level of 5 kPa followed by a recovery time of 120 seconds. After two such cycles of creep and recovery, the test specimen was subjected to a sinusoidal load with varying frequencies and stress amplitudes. Table 4.1 summarizes the stress amplitudes, frequencies and duration for which the load was applied. Note that at lower frequencies the stress amplitude was reduced to minimize damage to the specimen. Also a rest period of 120 seconds was allowed after each frequency. Finally, the complex modulus and phase angle were recorded only using the last few cycles at each frequency to minimize the influence of the initial transients. It is noted that although the complex modulus for the complete frequency spectra can be calculated using the principle of superposition with the data from the creep-recovery curve, these tests were conducted to provide a more robust estimation for the linear viscoelastic properties.

Cyclic tests to evaluate the fatigue cracking resistance were conducted by applying a sinusoidal torsion shear with a stress amplitude of 210 kPa at a frequency of 10 Hz.

**Table 4.1. Sequence of loading to obtain the complex modulus of the test specimens**

Step	Stress Amplitude (kPa)	Frequency (Hz)	Cycles
1	5	10	300
2	5	5	150
3	1	1	10
4	0.5	0.5	10

## 4.2 LINEAR VISCOELASTIC PROPERTIES

As described in section ??, the linear viscoelastic properties were obtained by conducting a creep-recovery test as well as a cyclic test following sinusoidal loading. The creep data could be reasonably described using the power law model:

$$J(t) = J_0 + J_1 t^m \quad (4.1)$$

where,  $J_1$ ,  $J_0$ , and  $m$  are material constants and  $t$  is time. Figures 4.1 and 4.2 summarize the  $J_1$  and  $m$  values for the four different mixes used in this study. Figure 4.3 compares the  $G^* \sin \delta$  parameter for the four mixes at two different test frequencies. Two observations are made from these results. First, results from this figure illustrate that the  $G^* \sin \delta$  parameter was very similar for all four mixes at the test temperature. This was expected considering that the four different binders used in these mixtures had a similar true grade (Table3.1). This also suggests, that the stress state of the binder within the glass bead specimen either had a no effect or a similar effect on the complex modulus of all four asphalt binders. Second, although the complex modulus, phase angle, and in particular the product of these two parameters were similar for the four mixes, the creep compliance properties of the four mixes were very different. This can be explained based on the fact that the complex modulus and phase angle represent properties at a single point in the frequency domain, whereas the creep compliance reflects the material response over a range of time span. It is also noted that the binders used in this study were specifically designed to meet the requirements based properties at a single point in the frequency domain, i.e. the  $G^* \sin \delta$  parameter.

As discussed previously, either the creep compliance (time domain) or the complex modulus from cyclic tests (frequency) can be used to estimate the linear viscoelastic properties of the test specimens. In this case, we conducted both tests to ensure the robustness of the linear viscoelastic properties that were subsequently used for damage analysis. Figures

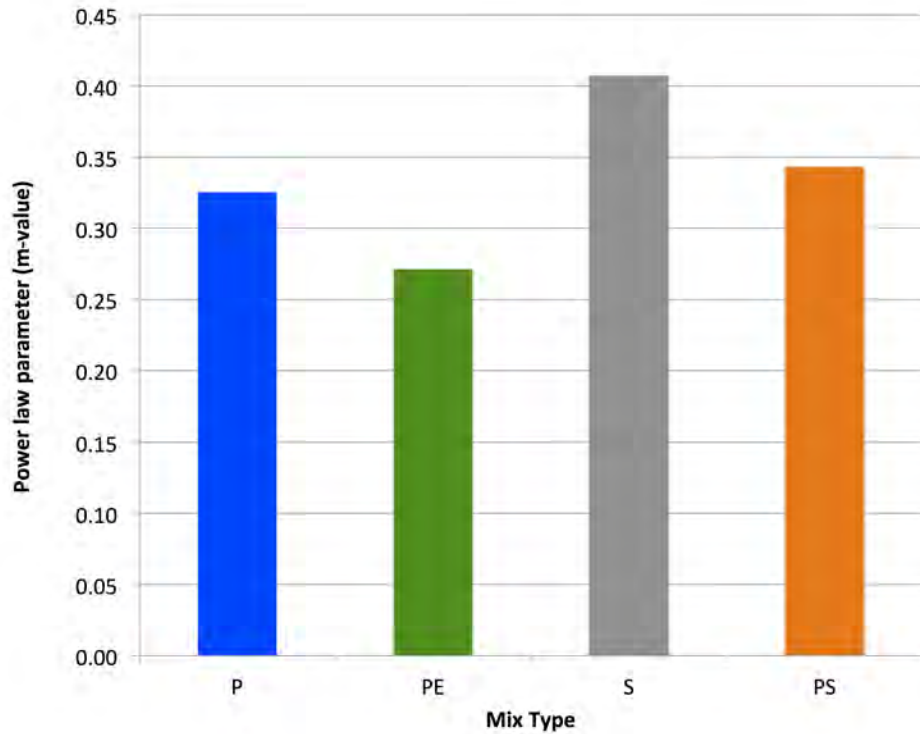


**Figure 4.1. Power law or m-value for the four different mixes**

4.4 and 4.5 compare the measured complex modulus and phase angle to the estimated complex modulus and phase angle using the creep compliance properties using the principle of linear superposition. Results from the figures indicate that the estimates were reasonable for data at higher frequencies as compared to data at lower frequencies. A further analysis of the data revealed that the lower stress amplitude used for lower frequencies of 1 Hz and 0.5 Hz (Table 4.1) resulted in very small deformation that was close to the limit of the instruments resolution. Another possibility for this discrepancy could be the nonlinear behavior of the material at very low stress amplitudes.

### **4.3 RESULTS FROM CYCLIC FATIGUE TESTS**

Cyclic tests were conducted by applying a sinusoidal torsion shear with a stress amplitude of 210 kPa at a frequency of 10 Hz until 300,000 cycles (500 minutes) or until specimen failure, whichever came first. All specimens with the exception of specimens fabricated using SBS modified binders failed within the 300,000 cycles limit. Results from the tests were

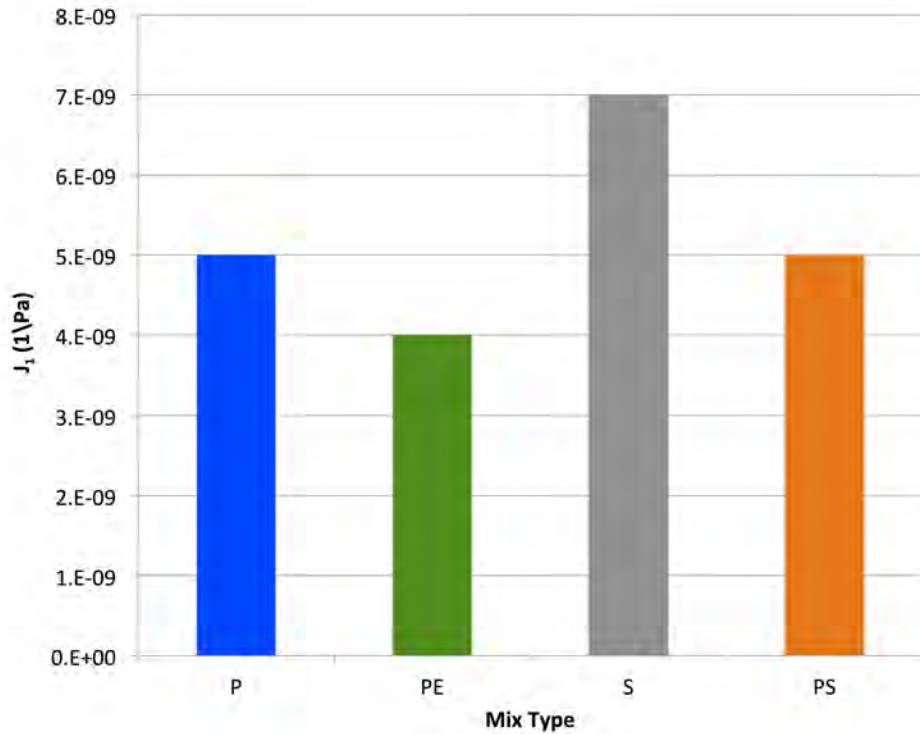


**Figure 4.2. Coefficient of power law or  $J_1$  for the four different mixes**

analyzed using a direct approach as well as the viscoelastic continuum damage method.

Figure 4.6 illustrates the range of results obtained from the cyclic tests for each of the four binder types. In all cases there were three distinct regions in the apparent modulus versus number of load cycles behavior: first, there was a precipitous reduction in the apparent modulus of the specimen, second the apparent modulus reduced at almost a steady rate (this is also where most of the load cycles until failure were consumed), finally the rate of reduction in the apparent modulus of the specimen increases significantly resulting in complete specimen behavior. Note that the last stage is not apparent when the test is conducted by applying a constant strain amplitude. The following approach was used to avoid subjectivity in identifying the total number of cycles to failure. A plot was generated for  $NG_N^*/G_1^*$  versus  $N$ , where  $G_N^*$  is the complex shear modulus at cycle  $N$  ((Kim and Little, 2005)). The number of load cycles corresponding to the maximum value of  $NG_N^*/G_1^*$  was then determined to be the number of load cycles to failure for the specimen (Figure 4.7). Figure 4.8 illustrates the number of load cycles to failure for the four different binder types that were tested in this study along with the range of maximum and minimum values.



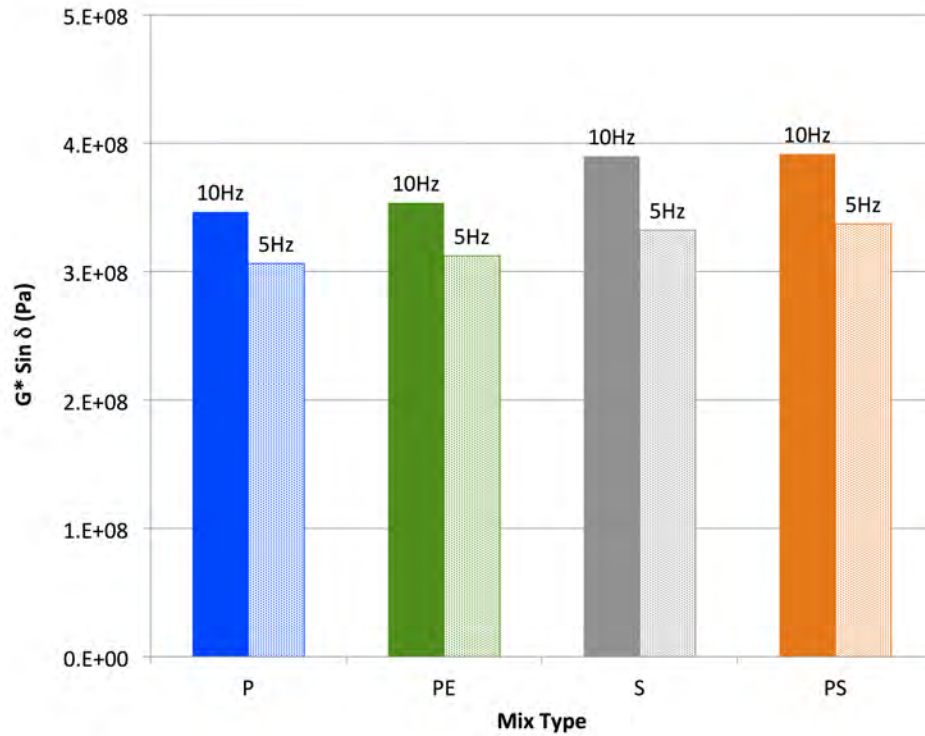


**Figure 4.3. Typical values of  $G^* \sin \delta$  for the four different mixes**

Fatigue cracking resistance of different materials can be compared directly based on the number of load cycles to failure when subjected to cyclic loading. However, a limitation of this approach is that in most cases the fatigue cracking resistance is defined by the specific test configuration (e.g. duration of the rest period, mode of loading, and loading frequency or amplitude). One approach to overcome this limitation is to use the work potential or viscoelastic continuum damage theory. Fatigue life of asphalt mixtures has been successfully characterized using work potential or viscoelastic continuum damage theory. Previous studies by Kim and co-workers (Park et al., 1996; Lee and Kim, 1998b,a; Daniel and Kim, 2002) provide significant evidence demonstrating that the viscoelastic continuum damage theory (VECD) can be used to characterize fatigue damage in an asphalt concrete mixture independent of the specific mode of loading or test conditions. The VECD theory relates the reduction in stiffness of a specimen subjected to cyclic loads to an internal state variable,  $S$ , that represents the overall damage within the specimen. This internal state variable is related to the loading and stiffness by a damage evolution law. Kim and co-workers demonstrated that the closed form relation between the pseudo stiffness  $C$  and

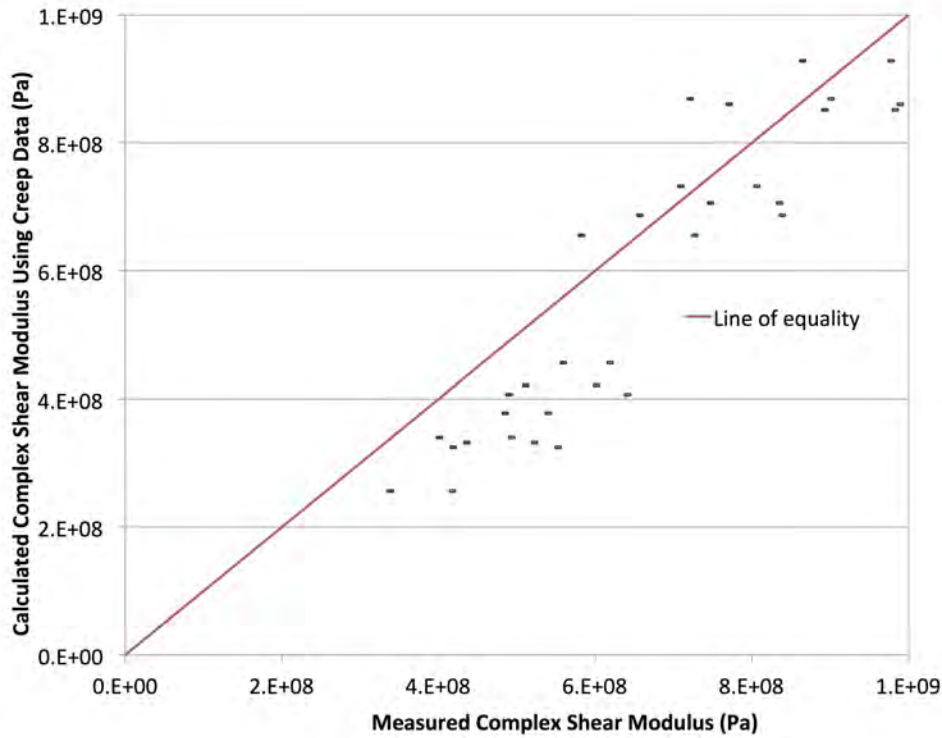


**Figure 4.4. Comparison of computed and measured complex modulus for different mixes and frequencies**

a damage parameter  $S$  was independent of the loading characteristics and unique for a particular material or mixture. The work potential or viscoelastic continuum damage theory that was used to further analyze the results from the cyclic tests is briefly described here.

The work potential theory developed by Schapery (1975) is a continuum damage theory that describes the mechanical behavior of an elastic material that experiences incremental damage using a damage evolution law derived from the principles of thermodynamics. Schapery (1975) demonstrated that a unique strain energy potential exists for a given material that can be used to represent its “state”. In this context, uniqueness implies that any mechanical, chemical or thermodynamic process that changes the material state from  $(S_1, \epsilon_1, \sigma_1)$  to  $(S_2, \epsilon_2, \sigma_2)$  requires the same amount of strain energy irrespective of the path, where  $S$ ,  $\epsilon$  and  $\sigma$  are defined as the thermodynamic internal state variable, strain and stress respectively. Schapery (1975; 1988) also demonstrated that the work potential theory or elastic continuum damage theory could be successfully extended to describe damage evolution in viscoelastic materials by using the correspondence principles and a

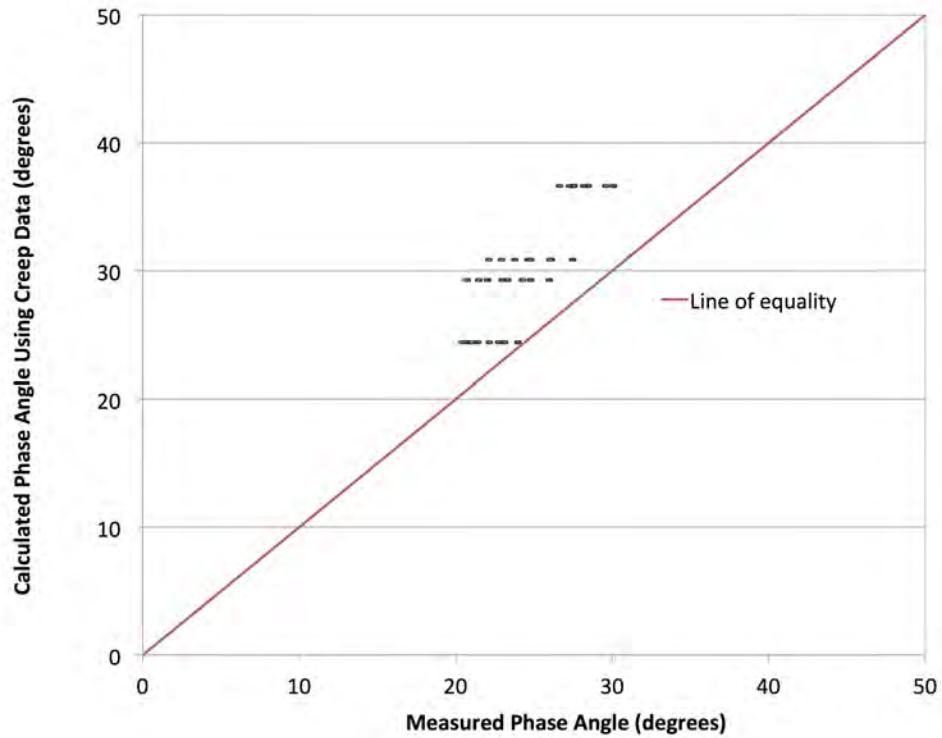


**Figure 4.5. Comparison of computed and measured phase angle for different mixes and frequencies**

new damage evolution law. Kim and co-workers used a similar approach to develop a viscoelastic continuum damage approach to characterize fatigue damage in asphalt mixtures (Park et al., 1996; Lee and Kim, 1998b,a; Daniel and Kim, 2002). They successfully used the VECD theory to develop a material function denoted by  $C(S)$  that relates the pseudo stiffness  $C$  of the material as a function of an internal state variable  $S$  that represents damage. This function represents the evolution of fatigue damage in asphalt mixtures. Most of these studies were conducted on full asphalt mixtures subjected to a cyclic tension or tension-compression mode. More recently, this theory was applied to characterize the fatigue cracking and healing characteristics of asphalt mortar specimens (asphalt binder and sand) subjected to cyclic shear (Palvadi et al., 2012).

The following procedure is typically used to characterize damage using the viscoelastic continuum damage theory. Correspondence principles are first used to transform the time dependent stress-strain data into a pseudo domain that corresponds to a hypothetical elastic material. In this study correspondence principle II or CP-II was used to transform stress and

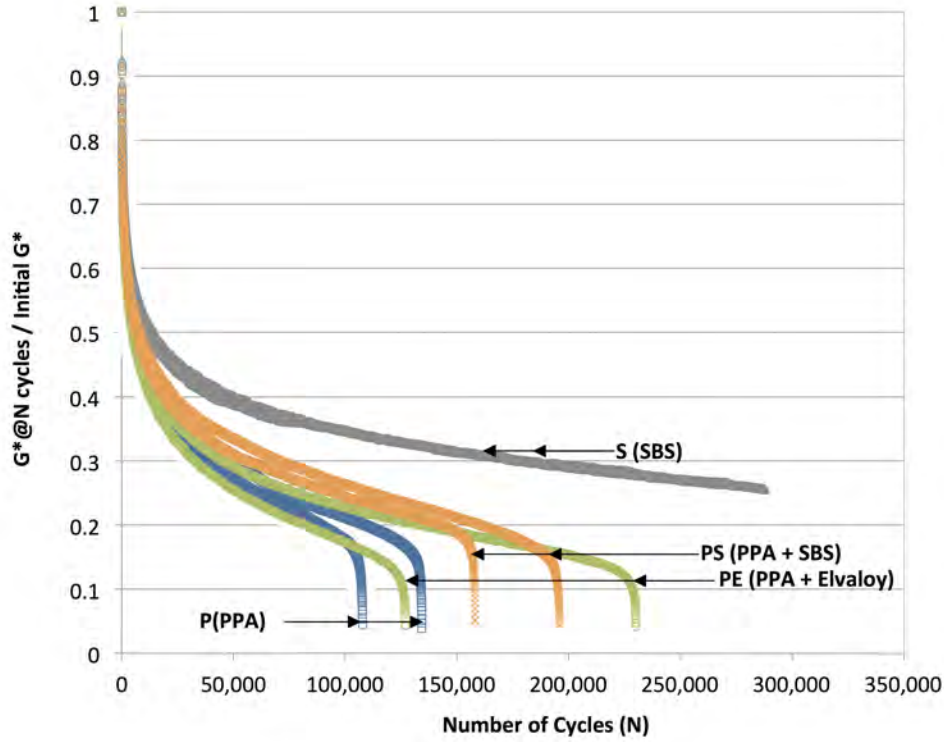


**Figure 4.6. Range of fatigue test results for each of the four binder types**

strain to pseudo stress and pseudo strain and eliminate time dependent effects (Schapery, 1975). According to CP-II, pseudo stress  $\sigma^R = \sigma$ ; where  $\sigma$  is the time dependent stress developed or applied to a viscoelastic material. Similarly, pseudo strain is given as:

$$\varepsilon^R = \frac{1}{E^R} \int_0^t E(t - \tau) \partial \varepsilon / \partial \tau d\tau \quad (4.2)$$

where  $\varepsilon$  is the time dependent strain in the viscoelastic material,  $E(t)$  represents the linear viscoelastic relaxation modulus of the material and  $E^R$  can be chosen to be any value that represents the modulus of the hypothetical elastic material. Lee and Kim (1998a) conducted a series of monotonic and cyclic load tests in both controlled stress and strain modes on asphalt concrete and concluded that pseudo stiffness  $C$ , defined as slope of  $\sigma^R$  versus  $\varepsilon^R$ , suitably reflects the evolution of damage in viscoelastic materials. Based on the pseudo stress-pseudo strain behavior of asphalt concrete subjected to simple uniaxial cyclic fatigue tests, they proposed the following constitutive model:

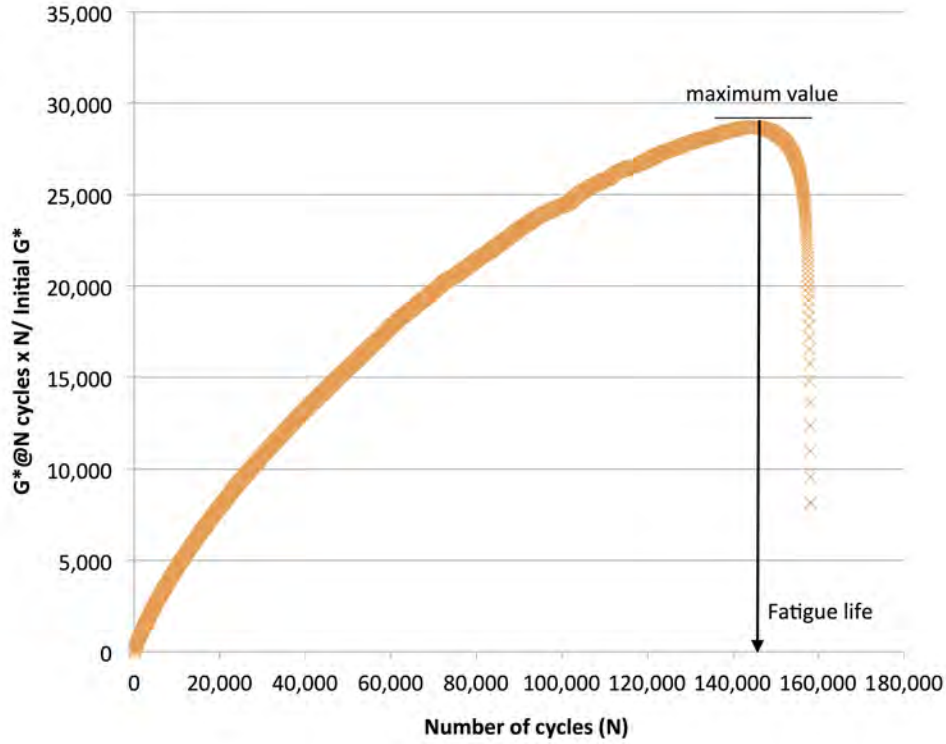


**Figure 4.7. Typical plot showing the determination of number of load cycles to failure**

$$\sigma^R = (F + G) \varepsilon^R I \quad (4.3)$$

The strain energy potential based on equation 4.3 was given as:

$$W^R = \frac{1}{2} (F + G) I (\varepsilon^R)^2 \quad (4.4)$$

where, the function  $F$  represents a factor that accommodates the change in pseudo stiffness, function  $G$  represents hysteretic behavior in pseudo stress- pseudo strain relationship, and  $I$  represents the initial pseudo stiffness, introduced to reduce specimen to specimen variability. A similar model can be adopted to characterize fatigue life in FAM mixes. In this study fatigue damage was characterized in terms of the loss in stiffness. The following forms of equations 4.3 and 4.4 were used:

$$\sigma^R = C(S) \varepsilon^R \quad (4.5)$$

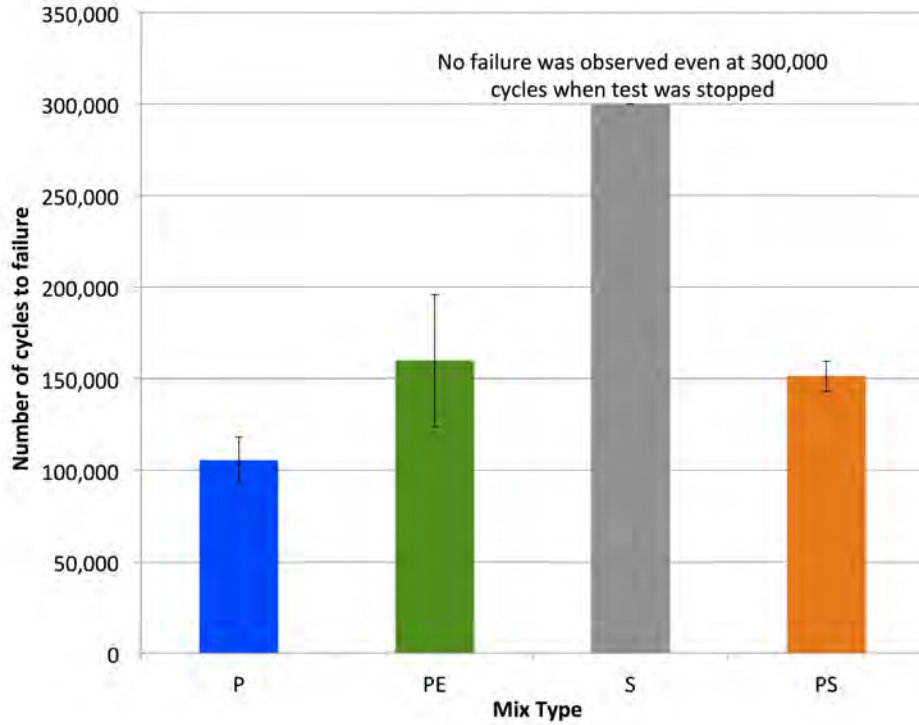


**Figure 4.8. Number of load cycles to failure along with maximum and minimum values from cyclic tests at 10Hz by applying a constant stress amplitude of 210 kPa**

$$W^R = \frac{1}{2}C(S) (\epsilon^R)^2 \quad (4.6)$$

where,  $C(S)$  represents the change in stiffness as a function of  $S$ , and represents the pseudo stress amplitude for cyclic tests and pseudo stress for monotonic tests. Similarly,  $\epsilon^R$  represents pseudo strain amplitude or pseudo strain depending on the type of test.

Schapery (1988) proposed a rate dependent damage evolution law, a variation of which was later developed by Lee and Kim (1998a) for asphalt mixtures. This simplified equation relating  $S$ ,  $\epsilon^R$  and  $C$  is given by:

$$S \approx \sum_{i=1}^n \left[ 0.5 (\epsilon^R)^2 (C_{i-1} - C_i) \right]^{\frac{\alpha}{1+\alpha}} (t_i - t_{i-1})^{\frac{1}{1+\alpha}} \quad (4.7)$$

In equation 4.7,  $\alpha$  is related to the material creep and is suggested to take values of  $(1 + 1/m)$  or  $(1/m)$  depending on the type of fracture, where  $m$  is the exponent of linear viscoelastic creep compliance. The value of  $(1/m)$  is theoretically applicable when the work of

fracture and size of the fracture process zone within the material are assumed to be constant, whereas the value of  $(1 + 1/m)$  is theoretically applicable when the mean tensile stress across the fracture zone is constant.

The above approach was used to obtain the characteristic damage evolution for the specimens with the four different binder types used in this study. The stress and strain were converted to pseudo variables using an approximate method for a cyclic load test with stress amplitude of  $\sigma_0$ , strain amplitude of  $\epsilon_0$  where the pseudo stress, pseudo strain and pseudo stiffness are given as:

$$\sigma^R = \sigma_0 \quad (4.8)$$

$$\epsilon^R = \epsilon^0 \frac{G_{LVE}^*}{G^R} \quad (4.9)$$

$$C_N = \frac{G_N^*}{G_{LVE}^*} \quad (4.10)$$

The notation  $C_N$  represents the estimate of the pseudo stiffness at cycle  $N$ . The damage evolution corresponding to the change in pseudo stiffness was determined by expressing equation 4.7 in terms cycles of loading instead of time. In a previous study, the aforementioned approximate method yielded reasonable results and the characteristic  $C(S)$  function was independent of the test method. Therefore this approximate method was used for further analysis. However, a more robust method that involves complete integration of the first few cycles to obtain the pseudo variables will be investigated in future work (Daniel and Kim, 2002). An exponential function, similar to the one used by Kutay et al. (2008), was found to fit the  $C$  versus  $S$  data determined for the four different damage evolution curves:

$$C = \exp(m_1 S^{m_2}) \quad (4.11)$$

The estimates for the material constants  $m_1$  and  $m_2$  for the four different binder types were determined using data from the different replicate tests. Figure 4.9 illustrates a typical  $C(S)$  for the test specimens using the PPA modified binder. The characteristic  $C(S)$  for each binder type was then be used to estimate the fatigue cracking characteristics of the material (the glass bead - binder composite in this case) under different loading configurations. In this study, this analysis was primarily conducted to estimate the expected number of load cycles for the test specimen to reach 50% of its initial modulus when subjected to a cyclic

load with a constant strain amplitude and compare these results to similar results from mixture testing reported in the literature.

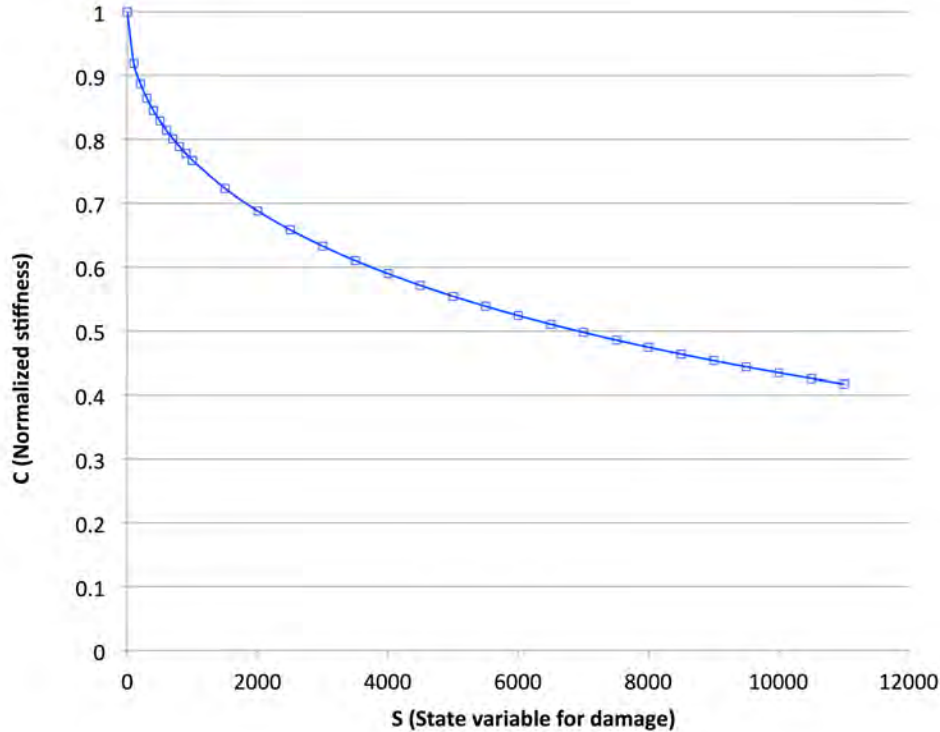


**Figure 4.9. Typical damage evolution curve (C vs S) for a binder type**

## 4.4 DISCUSSION OF RESULTS

### 4.4.1 Comparison to mixture performance data

Figure 4.6 illustrates that the four different asphalt binders have distinctly different fatigue cracking performance at the intermediate temperature. This is despite the fact that these binders were rated to have a very similar true performance grade based on the current Superpave binder specifications. Figure 4.10 illustrates the results from cyclic fatigue tests conducted on full asphalt mixtures fabricated using these four asphalt binders. These tests were conducted by applying cyclic loads and tension-compression with a constant cross head amplitude on the loading frame. The results illustrated in Figure 4.10 do not indicate the loss of modulus in a truly strain controlled or stress controlled mode of loading. These results must be processed through the continuum damage model to obtain the true failure



characteristics of the materials. Nevertheless, a qualitative comparison between the results from the tests conducted on full asphalt mixtures (Figure 4.10) and the tests conducted on the glass bead - binder specimens (Figure 4.6) can be made. More notably, first, the PPA modified binder and the SBS modified binder resulted in the two extreme ends in terms of the performance. Second, all binders demonstrated a precipitous reduction in modulus during the first few cycles. This comparison demonstrates the ability of the glass bead - binder composite specimen to evaluate the fatigue cracking characteristics of the binder when treated as a soft matrix with rigid particle inclusions.

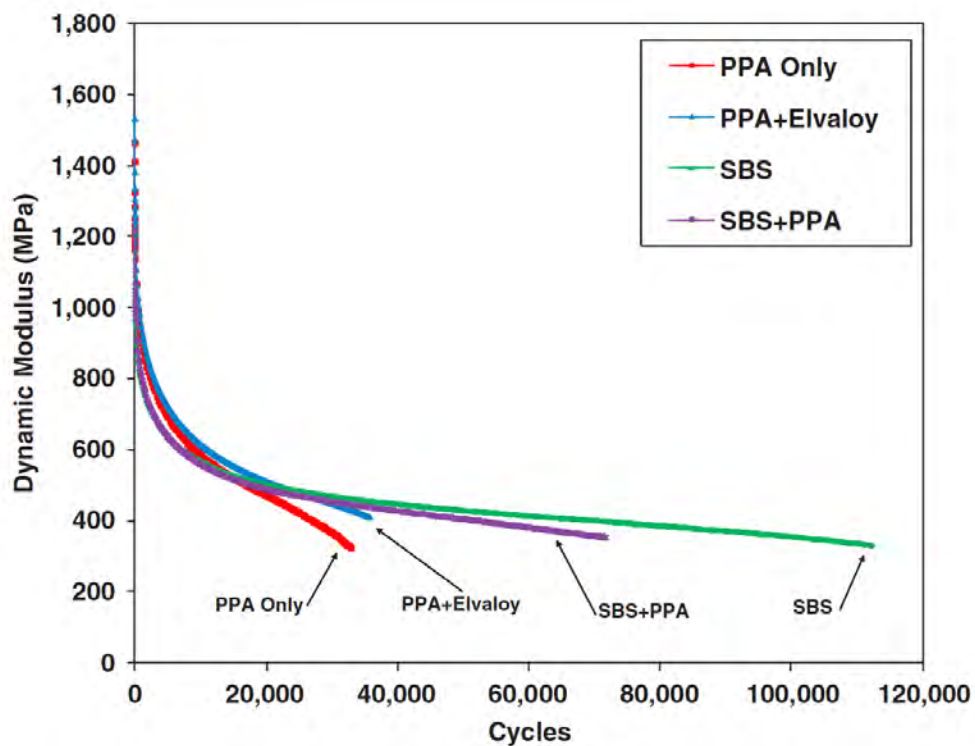


**Figure 4.10. Fatigue cracking characteristics of full asphalt mixtures using the four different binders**

(From Li et al. 2011, Figure 1, p.53. Copyright, National Academy of Sciences, Washington, D.C., 2011. Reproduced with permission of the Transportation Research Board)

As mentioned above, the results reported by Li et al. (2011) included both direct measurements from the cyclic tests (Figure 4.10) as well as computed load cycles to reach 50% of the initial modulus when subjected to a true strain amplitude controlled cyclic load test. The latter was obtained from the viscoelastic continuum damage analysis of the mixture test results. A similar analysis was also conducted for the results obtained from the test-

ing of the glass bead - binder composite specimens in this study. Figure 4.11 illustrates a comparison of the calculated number of load cycles to reach 50% modulus for the full asphalt mixtures (Li et al. 2011) and for the glass bead - binder specimen used in this study. This comparison again illustrates that there was a reasonable agreement in the rank order of the number of load cycles to reach 50% of initial modulus for the mixtures and glass bead specimens that incorporated the four modified binders.

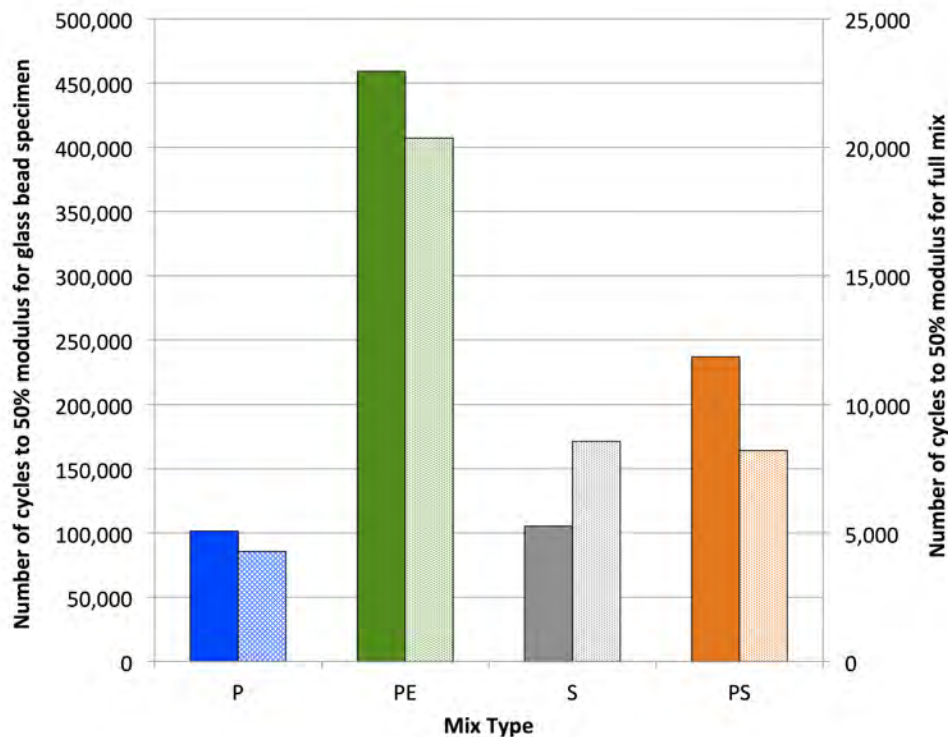


**Figure 4.11. Comparison of calculated number of load cycles to reach 50% of initial modulus for a cyclic test at 10Hz by applying a constant strain amplitude for binder (left) and mixture (right)**

(Results for mixture performance were adapted from Li et al. 2011, Figure 12, p.55. Copyright, National Academy of Sciences, Washington, D.C., 2011. Reproduced with permission of the Transportation Research Board)

#### 4.4.2 Failure criterion

One important observation that can be made from both the mixture as well as the glass bead specimen test data is the loss in modulus of the test specimen with respect to the number of

load cycles. In all cases, the test specimens experienced a 50% loss in the initial modulus of the composite in less than 5% of the actual number of load cycles to failure. In other words, a failure criterion of 50% loss in initial modulus can significantly underestimate the true fatigue cracking life of the specimen. Three additional comments can be made on this observation.

First, one may argue that 50% of the initial modulus can in fact still be used as a failure criterion because the material has significantly lost its ability to resist deformation when subjected to external loads. This may be a valid consideration but it would require addressing the definition of failure at both the material and structural level, which was beyond the scope of this report.

Second, based on similar tests conducted in other studies by one of the authors, unmodified binders tend to have a much smaller difference between the number of load cycles to failure based on the 50% modulus loss criterion and the true specimen failure. For example, Figure 4.12 illustrates the loss in modulus of a sand-asphalt or fine aggregate matrix specimen when subjected to cyclic shear. The results in this figure were fairly typical for several unmodified asphalt binders in the sense that the true specimen failure typically occurred when the specimen was close to 50% of its initial modulus.

Third, Figure 4.12 compares the number of cycles to achieve 50% loss in modulus of the full asphalt mixture to the glass bead specimens. This comparison was made only to evaluate the ability of using the glass bead specimens for binder characterization. The results in this figure may not reflect the rankings of the mixtures or binders in terms of their true fatigue cracking resistance.

#### **4.4.3 Other notes**

The results above compare the performance of the glass bead - binder composite to the performance of the full asphalt mixtures. The authors recognize that in most cases such a direct comparison may not be feasible on account on several reasons. This is because mixture properties (eg. aggregate gradation, binder content) can significantly influence the results and also because typically mixture tests are conducted only on short-term aged specimens whereas the proposed test method was conducted on long-term aged binder. Nevertheless, it is important to evaluate the fatigue cracking characteristics of the asphalt binder in order to assess its inherent ability to resist fatigue cracking. This is even more important in the context of evaluating modifiers and additives that are increasingly being introduced in the industry in order to improve binder performance.

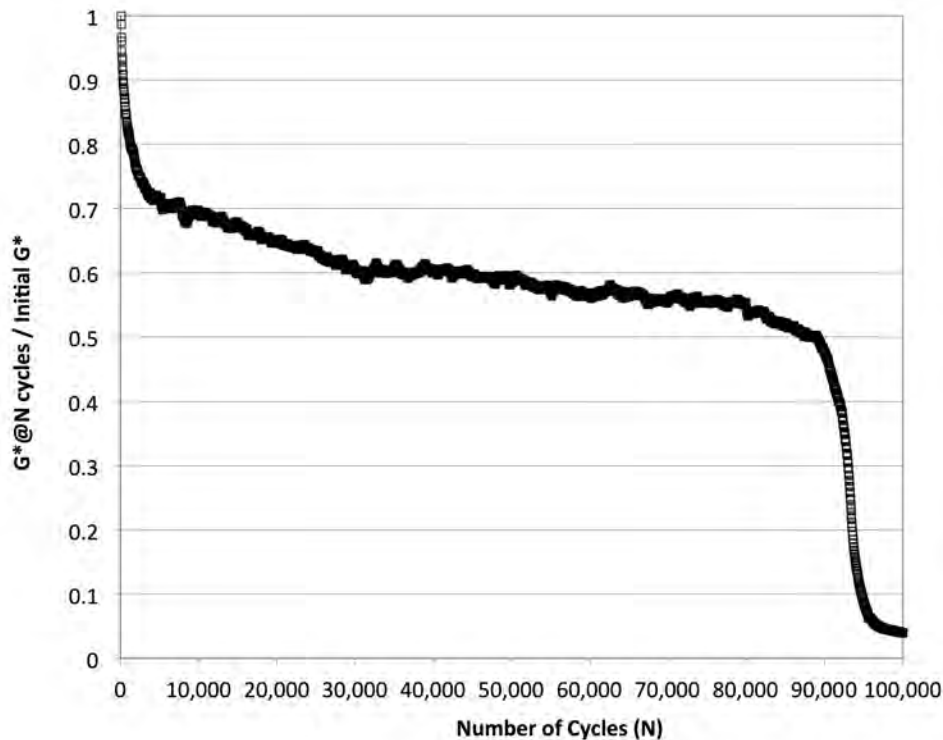


**Figure 4.12. Loss in modulus as a function of number of load cycles applied for a fine aggregate matrix with unmodified PG 58-22 asphalt binder**

The approach used in this study was to evaluate the fatigue cracking resistance of asphalt binders subjected to cyclic loading when treated as a soft matrix with rigid inclusions. In fact, several previous studies have used fine aggregate matrix (or sand asphalt mortars) to successfully evaluate and compare the impact of binders and modifiers on the fatigue cracking resistance of the matrix (Kim et al., 2003; Masad et al., 2006b,a; Caro et al., 2008). The proposed approach using a gradation of glass beads helps eliminate the variability and potential for physio-chemical interactions due to the use of fine mineral aggregates, especially in cases when the properties of the binder (or a binder with a modifier) are of interest. From the point of view of routine use for specification purposes at a transportation agency, the approach presented in this report may require relatively more time compared to other alternative test methods such as the Linear Amplitude Sweep Test (Bahia et al., 2010) that are currently being evaluated. However, this approach can be used to supplement DSR based tests to more rigorously evaluate the inherent fatigue cracking resistance of modified and unmodified asphalt binders or even fillers subjected to an appropriate stress state.

## CHAPTER 5. CONCLUSIONS

The following are some of the main conclusions from this study.

1. A test method to evaluate the inherent fatigue cracking resistance of asphalt binders in the form of a matrix with rigid inclusions was investigated. The test method utilizes long-term aged (using a pressure aging vessel) binders, which is more critical for fatigue cracking resistance. The test method was sensitive to distinguish between the fatigue cracking resistance of four different asphalt binders.
2. Results demonstrate that four asphalt binders modified using different methods had different fatigue cracking resistance despite the fact that these four binders were rated to have very similar temperature grade based on the Superpave specifications.
3. Fatigue cracking characteristics of the glass bead - binder test specimens used in this study were qualitatively very similar to the fatigue cracking characteristics of full asphalt mixtures using the same binders. The rank order of fatigue cracking resistance for the four glass bead - binder mixtures compared reasonably well to the rank order of fatigue cracking resistance for the full asphalt mixtures that incorporated these asphalt binders.
4. The true failure of the test specimens occurred when the complex modulus of the specimen was much lower than 50% of its initial complex modulus. In fact, all test specimens reached 50% of their fatigue life at less than 5% of the cycles required for complete failure. This was also true of the results reported in another study using these four binders based on tests conducted on full asphalt mixtures (Li et al., 2011).

--- DRAFT ---

## REFERENCES

- Anderson, D., Hir, Y., Marasteanu, M., Planche, J., Martin, D., and Gauthier, G. 2001. Evaluation of fatigue criteria for asphalt binders. *Transportation Research Record: Journal of the Transportation Research Board*, 1766(-1):48–56.
- Andriescu, A. and Hesp, S. A. 2009. Time-temperature superposition in rheology and ductile failure of asphalt binders. *International Journal of Pavement Engineering*, 10(4):229–240.
- Arega, Z., Bhasin, A., Motamed, A., and Turner, F. 2011. Influence of Warm-Mix additives and reduced aging on the rheology of asphalt binders with different natural wax contents. *Journal of Materials in Civil Engineering*, 23(10):1453.
- Bahia, H. U., Wen, H., and John, C. 2010. Developments in intermediate temperature binder fatigue specifications. In *Development of asphalt binder specifications*, number E-C147 in Transportation Research Circular, pages 25–33. Transportation Research Board, Washington, D.C.
- Bhasin, A., Masad, E., Little, D. N., and Lytton, R. 2006. Limits on adhesive bond energy for improved resistance of Hot-Mix asphalt to moisture damage. *Transportation Research Record: Journal of the Transportation Research Board*, 1970:3–13.
- Caro, S., Masad, E., Airey, G. D., Bhasin, A., and Little, D. N. 2008. Probabilistic analysis of fracture in asphalt mixtures caused by moisture damage. *Transportation Research Record*, 2057(1):28–36.
- Cristiano, A., Marcellan, A., Long, R., Hui, C., Stolk, J., and Creton, C. 2010. An experimental investigation of fracture by cavitation of model elastomeric networks. *Journal of Polymer Science Part B: Polymer Physics*, 48(13):1409–1422.
- D’Angelo, J. 2010. New high temperature binder specification using multistress creep and recovery. In *Development of asphalt binder specifications*, number E-C147 in Transportation Research Circular, pages 1–13. Transportation Research Board, Washington, D.C.

- D'Angelo, J., Kluttz, R., Dongre, R., Stephens, K., and Zanzotto, L. 2007. Revision of the superpave high temperature binder specification: The multiple stress creep recovery test. *Journal of the Association of Asphalt Paving Technologist*, 76.
- Daniel, J. S. and Kim, Y. R. 2002. Development of a simplified fatigue test and analysis procedure using a viscoelastic, continuum damage model. *Journal of the Association of Asphalt Paving Technologist*, 71.
- Elseifi, M., Al-Qadi, I., Yang, S., and Carpenter, S. 2008. Validity of asphalt binder film thickness concept in Hot-Mix asphalt. *Transportation Research Record: Journal of the Transportation Research Board*, 2057:37–45.
- Fee, D., Martin, J., Reinke, G., and Clyne, T. R. 2008. Polyphosphoric acid modified asphalt in conjunction with lime as an antistripping agent. In *Petersen Conference*, Wyoming.
- Fond, C. 2001. Cavitation criterion for rubber materials: A review of void growth models. *Journal of Polymer Science Part B: Polymer Physics*, 39(17):2081–2096.
- Gent, A. N. and Lindley, P. B. 1959. Internal rupture of bonded rubber cylinders in tension. *Proceedings of the Royal Society of London. Series A, Mathematical and Physical Sciences*, 249(1257):195–205. ArticleType: research-article / Full publication date: Jan. 1, 1959 / Copyright © 1959 The Royal Society.
- Harvey and Cebon 2003. Failure mechanism in viscoelastic films. *Journal of Materials Science*, 38:1021–1032.
- Hom, C. L. and McMeeking, R. M. 1991. Plastic flow in ductile materials containing a cubic array of rigid spheres. *International Journal of Plasticity*, 7(4):255 – 274.
- Johnson, C. 2010. *Estimating asphalt binder fatigue resistance using an accelerated test method*. Ph.D. dissertation, University of Wisconsin at Madison, Madison, WI.
- Kim, Y. and Little, D. N. 2005. Development of specification type tests to assess the impact of fine aggregate and mineral filler on fatigue damage. Technical Report 0-1707-10, Texas Transportation Institute.
- Kim, Y. R., Little, D. N., and Song, I. 2003. Effect of mineral Fillers on fatigue resistance and fundamental material characteristics: Mechanistic evaluation. *Transportation Research Record: Journal of the Transportation Research Board*, 1832:1–8.



- Kutay, E. M., Gibson, N., and Youtcheff, J. S. 2008. Conventional and viscoelastic continuum damage (VECD) based fatigue analysis of polymer modified asphalt pavements. *Journal of the Association of Asphalt Paving Technologist*.
- Lee, H. and Kim, Y. R. 1998a. Viscoelastic constitutive model for asphalt concrete under cyclic loading. *Journal of engineering mechanics*, 124(1):32–40.
- Lee, H. J. and Kim, Y. R. 1998b. Viscoelastic continuum damage model of asphalt concrete with healing. *Journal of engineering mechanics*, 124(11):1224–1232.
- Li, X., Clyne, T. R., Reinke, G., Johnson, E. N., Gibson, N., and Kutay, E. M. 2011. Laboratory evaluation of asphalt binders and mixtures containing polyphosphoric acid. *Transportation Research Record: Journal of the Transportation Research Board*, 2210:47–56.
- Li, X., Williams, R. C., Marasteanu, M. O., Clyne, T. R., and Johnson, E. 2009. Investigation of In-Place asphalt film thickness and performance of Hot-Mix asphalt mixtures. *Journal of Materials in Civil Engineering*, 21(6):262–270.
- Lindsey, G. H. 1967. Triaxial fracture studies. *Journal of Applied Physics*, 38(12):4843–4852.
- Marek, C. R. and Herrin, M. 1968. Tensile behavior and failure characteristics of asphalt cements in thin films. *Journal of the Association of Asphalt Paving Technologist*, 37:386–421.
- Masad, E., Branco, V. C., and Little, D. N. 2006a. Fatigue damage: Analysis of mastic fatigue damage using stress controlled and strain controlled test. Technical Report 473630, Texas Transportation Institute in cooperation with Federal Highway Administration and Western Research Institute.
- Masad, E., Howson, J. E., Bhasin, A., Caro, S., and Little, D. N. 2010. Relationship of ideal work of fracture to practical work of fracture. *Journal of the Association of Asphalt Paving Technologist*, 79(In Press).
- Masad, E., Zollinger, C., Bulut, R., Little, D. N., and Lytton, R. L. 2006b. Characterization of HMA moisture damage using surface energy and fracture properties. *Proc. Association of Asphalt Paving Technologists*, 75:713–754.

- Olard, F. and Di Benedetto, H. 2004. Fracture toughness and fracture energy of bituminous binders at low temperatures. In *Proceedings, 5th International RILEM Conference*, pages 359–366, Limoges, France.
- Palvadi, S., Bhasin, A., and Little, D. N. 2012. A method to quantify healing asphalt composites using continuum damage approach. *Transportation Research Record: Journal of the Transportation Research Board*, In Press.
- Park, S. W., Richard Kim, Y., and Schapery, R. A. 1996. A viscoelastic continuum damage model and its application to uniaxial behavior of asphalt concrete. *Mechanics of Materials*, 24(4):241–255.
- Planche, J., Anderson, D. A., Gauthier, G., Le Hir, Y. M., and Martin, D. 2004. Evaluation of fatigue properties of bituminous binders. *Materials and Structures*, 37:356–359.
- Poulikakos, L. and Partl, M. 2010. Micro scale tensile behaviour of thin bitumen films. *Experimental Mechanics*, pages 1–13.
- Reinke, G. 2010. Use of hamburg rut testing data to validate the use of jnr as a performance parameter for high-temperature permanent deformation. In *Development of asphalt binder specifications*, number E-C147 in Transportation Research Circular, pages 14–24. Transportation Research Board, Washington, D.C.
- Schapery, R. A. 1975. A theory of crack initiation and growth in viscoelastic media, III. analysis of continuous growth. *International Journal of Fracture*, 11(4):549–562.
- Schapery, R. A. 1988. On viscoelastic deformation and failure behavior of composite materials with distributed flaws. In Wang, S. S. and Renton, W. J., editors, *Advances in Aerospace Structures and Materials*, volume AD-01, pages 5–20.
- Sherwood, J., Thomas, N., and Qi, X. 1998. Correlation of superpave  $G^*/\sin \dot{\epsilon}$  with rutting test results from accelerated loading facility. *Transportation Research Record: Journal of the Transportation Research Board*, 1630(-1):53–61.